uOttawa

L'Université canadienne
Canada's university

FACULTÉ DES ÉTUDES SUPÉRIEURES ET POSTOCTORALES

uOttawa

L'Université canadienne
Canada's university

FACULTY OF GRADUATE AND POSDOCTORAL STUDIES

Joshua Yee Sing Chang
AUTEUR DE LA THÈSE / AUTHOR OF THESIS

M.Sc. (Biochemistry)
GRADE / DEGREE

Department of Biochemistry, Microbiology and Immunology
FACULTÉ, ÉCOLE, DÉPARTEMENT / FACULTY, SCHOOL, DEPARTMENT

Porphyromonas Gingivalis and the Participatory Role of Interleukin-1 β in the Progression of Atherosclerosis

TITRE DE LA THÈSE / TITLE OF THESIS

Ross Milne
DIRECTEUR (DIRECTRICE) DE LA THÈSE / THESIS SUPERVISOR

CO-DIRECTEUR (CO-DIRECTRICE) DE LA THÈSE / THESIS CO-SUPERVISOR

Daniel Sparks

Xiaohui Zha

Gary W. Slater
Le Doyen de la Faculté des études supérieures et postdoctorales / Dean of the Faculty of Graduate and Postdoctoral Studies

Porphyromonas gingivalis and the Participatory Role of Interleukin-1β in the Progression of Atherosclerosis

Joshua Y.S. Chan, BSc

Supervised by the late Dr. Stewart C. Whitman, PhD
Co-supervised by Dr. Ross W. Milne, PhD

A thesis submitted in partial fulfillment of
the requirements for the degree of
Master of Science, Biochemistry
Dept. of Biochemistry, Microbiology & Immunology,
Faculty of Medicine, University of Ottawa, Ottawa, ON CANADA

June 25th 2010

Your file Votre référence
ISBN: 978-0-494-73801-6
Our file Notre référence
ISBN: 978-0-494-73801-6

Abstract

Periodontal disease promotes atherosclerosis via a poorly defined mechanism. Our laboratory has previously shown that caspase-1, responsible for activating IL-1β, is important in this process. We hypothesized that *Porphyromonas gingivalis* infection requires activated IL-1β to promote atherosclerosis. Six-week old IL-1β-/- apoE-/- mice of both genders received 15 oral inoculations of *P.gingivalis*. Detection of anti-*P.gingivalis* antibodies in serum of inoculated mice confirmed successful infection. Unexpectedly, atherosclerosis at age 17 weeks showed no effect of infection on IL-1β+/+ mice. Moreover, contrary to our hypothesis, inoculated IL-1β-/- females showed increased rather than decreased atherosclerosis compared to inoculated IL-1β+/+ and non-inoculated IL-1β-/-. Thus, either IL-1β does not play a role in atherosclerosis development following *P.gingivalis* infection or there is a compensatory mechanism. IL-1β deficiency may stimulate another pathway to promote *P.gingivalis*-induced atherosclerosis. Elucidation of the pathway by which *P.gingivalis* infection contributes to atherosclerosis development could reveal novel targets for therapy to impede disease progression.

Table of Contents

List of Figures

Abbreviations Used

ABCA-1 – ATP binding cassette A-1
ABCG-1 – ATP binding cassette G-1
ASC – apoptosis speck like protein containing CARD domain
ANOVA – analysis of variance
apoE – apolipoprotein E
CARD – Caspase recruitment Domains
CETP – cholesterol ester transfer protein
CVD – Cardiovascular disease
ELISA – enzyme linked immunosorbent assay
HDL – high density lipoproteins
ICE – Interleukin-1beta converting enzyme a.k.a. Caspase-1
IDL – intermediate density lipoproteins
IL-1β – Interleukin-1 beta
IPAF – ICE protease activating factor
IRAK - IL-1R-associated kinase
LCAT – Lecithin cholesterol acyltransferase
LDL – low density lipoproteins
LDLR – LDL receptor
LpL – Lipoprotein Lipase
LPS – Lipopolysaccharide
NF-κB - nuclear factor –κB
PAMP – pathogen associated molecular pattern
PCR – Polymerase Chain Reaction
PRR - pattern recognition receptor
OD – Optical Density
TG – Triacylglycerol or triglyceride
TLR – Toll Like Receptor
TLR2 – Toll Like Receptor 2
TLR4 – Toll Like Receptor 4
TNFα – Tumor Necrosis Factor α
VLDL – very low density lipoproteins

Acknowledgements

So many people have helped me out in countless ways, however big and small, over the course of my time in the Whitman Lab and I do not believe this undertaking would have been successful without their help. I must start off with none other than the late Dr. Stewart Whitman, who graciously took me under his wing and gave me an opportunity to spread mine. I feel very blessed to have had the opportunity to know Dr. Whitman. The determination and fight that he put up against his illness was out of this world. He really was an inspiration for us and will be sorely missed. I will never forget seeing his face, just hours before he passed on, watching him struggle to speak, wishing I could do more to help. A huge thank you goes to Dr. Ross Milne for graciously helping co-supervise me when Dr. Whitman's health was making it difficult for him to do it alone and for all the support following Dr. Whitman's passing. My thesis advisory committee, Drs. Frans Leenen and Kathryn Wright, thank you for all the input, suggestions and guidance. The Whitman lab technicians that I had the chance to work with: Sarah Burchat, Jessica Gage, Mirela Hasu, & Mohamed Thabet, thanks for all of your help, teaching me everything around the lab, and for sharing your humour and life experiences with me. Various members of the Whitman Lab for their input, support and humour along the way: Justin Caravaggio, Lindsay Willcox, Ali Ahmadi, Robin MacLaren, Caroline Klicius, Maria Campos, Razvan Matt Dobre, & Roxana Mititelu. A big thank you goes to Dr. Marc Desjardins and Marie Burelle for their help with microbiology diagnostics. I would like to extend my appreciation to Dr. Syed Sattar and Richard Kibbee for sharing their expertise in bacterial handling techniques. Having little experience in statistics, thank you Kathryn Williams and Robbie Davies for your expertise and assistance in helping me understand the statistical analyses of my data. It never hurts to have a friend you can count on to be in the lab next door late at night and on weekends to help with anything from editing abstracts to sharing a laugh over some "expired but it's still good cause we're grad students food" with: the one and only Josh Raizman. Of course I cannot forget the continued love and support I received from my parents. Last but definitely not least, thank you Jesus Christ, my Saviour and my God, for carrying me through it all –the ups and the downs. "I never said it would be easy, I only said I'd pull you through." It has been nothing less than an experience of a lifetime.

1. Introduction

1.1. Cardiovascular disease

Cardiovascular disease, which includes heart attacks and stroke, is currently responsible for the highest number of deaths in developed countries and is gaining ground in developing countries. In the United States alone, cardiovascular disease affects 36.9% of the population (Lloyd-Jones et al., 2010). Well known risk factors include elevated cholesterol levels, tobacco use, hypertension, physical inactivity, obesity, and diabetes. The main underlying cause of cardiovascular disease is the narrowing of the inner diameter of the arteries (and not by vasoconstriction), otherwise known as atherosclerosis. The development of atherosclerosis lies in the accumulation of modified low density lipoprotein (LDL) cholesterol molecules engulfed by macrophages within the arterial wall. This process will be discussed in further detail in a later section. Between 30-50% of heart disease cases however cannot be attributed to these aforementioned known risk factors. Within the unknown or lesser known risk factors is periodontal disease, which has been suggested many years ago based on observations in canines. The mechanism of how this risk factor exacerbates cardiovascular disease is however not well understood.

1.2. Lipoprotein metabolism

1.2.1. Lipoproteins and apolipoproteins

Plasma lipoproteins are molecules that transport hydrophobic water-insoluble lipids to and from peripheral tissues around the body. These water-insoluble lipids include cholesterol, triacylglycerol (TG, commonly known as triglyceride) and cholesterol ester. Most lipoproteins are generally spherical, comprised of a phospholipid monolayer with interspersed cholesterol molecules that surrounds a hydrophobic core of the neutral lipids, cholesteryl ester and triacylglycerol. There are five classes of lipoproteins: chylomicrons, very low density lipoproteins (VLDL), intermediate density lipoproteins (IDL), low density lipoproteins (LDL), and high density lipoproteins (HDL). The classification of lipoproteins into chylomicrons, VLDL, LDL, IDL, and HDL is based on their hydrated density. This hydrated density is a function of the lipid to protein ratio. Chylomicrons carry 1-2% of their weight as protein while HDLs owe approximately 50% of their weight to protein. Apolipoproteins are proteins found on the surface of lipoproteins and they serve several critical functions. They are responsible for dissolving water-insoluble lipids for transportation. These unique protein components of lipoproteins determine their assembly, structure, and metabolism. There are six different apolipoprotein classes (A, B, C, D, E, H) with several subclasses. Apolipoprotein (apo) A for example, can be sub-classified as A-I, A-II, A-IV or A-V. ApoA-I is the main protein component of HDLs whereas full length apolipoprotein B (apo B100) is the principle protein of LDLs. In addition to their structural role, specific apolipoproteins can also mediate the docking of lipoproteins to cell

surface lipoprotein receptors (apoE and apoB100) and can serve as co-factors for enzymes involved in lipoprotein metabolism e.g. apoA-I for LCAT, apoC-II for LPL).

Chylomicrons are assembled in, and secreted by intestinal enterocytes and have a density of 0.93g/ml and a diameter between 75-1200 nm. They exist in three different stages, beginning as nascent chylomicrons, becoming mature chylomicrons, and finally chylomicron remnants. These chylomicrons consist of a neutral lipid core, made of primarily triacylglycerols (TG) and some cholesteryl esters (CE) encompassed by a monolayer of phospholipids, unesterified cholesterol and apolipoproteins (Vance and Adeli, 2008). The apolipoproteins that can be found on the chylomicron at the different stages include apoA-I, apoA-II, apoA-IV, apoB-48, apoC-II, and apoE.

VLDLs are secreted by hepatocytes and have a density of 0.93 to 1.006 g/ml, a diameter of 30- 80nm and they carry endogenously synthesized TGs. The apolipoproteins that are found on VLDLs include a single molecule of apoB-100 and varying amounts of apoE, apoC-II, and apoC-III. These VLDLs later become VLDL remnants, which are also known as IDLs. IDLs have a density between 1.006 and 1.019 g/ml and a diameter of 25-35nm. They carry CE and TG as well as apolipoproteins such as apoB-100, apoE, apoC-II and apoC-III. IDLs can eventually become LDLs, which then have a density between 1.019 and 1.063 g/ml, a diameter of 18-25nm and they are found to be carrying predominantly CE and apoB-100.

A critical component of reverse cholesterol transport, HDLs have a density greater than 1.063g/ml and have different shapes based on differing proportions of cholesterol and protein content. HDL can be disc shaped (discoidal) or spherical and this mostly depends on the presence of CE to form the core of the spherical particle. Plasma enzyme lecithin cholesterol acyltransferase (LCAT) esterifies the free cholesterol in discoidal HDL particles and the HDL becomes spherical with the CE forming the neutral lipid core. HDL particles contain phospholipid, apoA-I, apoA-II, apoC-II, and apoE. This HDL is formed in the liver and intestine and it interacts with chylomicron remnants & LCAT. LCAT modifies discoidal HDL into the spherical HDL3 and eventually into HDL2a. HDL3 contains cholesterol, CE and phospholipids, in addition to apoA and apoE while HDL2a contains high concentrations of apoE and CE. With the help of the cholesterol ester transfer protein (CETP), HDL2a transfers CE to VLDL while VLDL transfers TG to the HDL2a molecule which becomes HDL2b. HDL2 can be converted into HDL3 with the help of hepatic lipase that hydrolyzes TG (Breslow, 1995).

1.2.2. Forward and reverse cholesterol transport

In the postprandial state, the intestine routes dietary fat into the lymphatic system and it subsequently makes its way into the blood stream to reach peripheral tissues. Three fatty acids are re-esterified onto a glycerol backbone in the intestinal enterocytes and are transferred to the apoB-48 carrying chylomicron (Green and Glickman, 1981). Flowing through lymphatic vessels, chylomicrons arrive at the thoracic duct and enter into the circulatory system via the left subclavian vein. During this time, chylomicrons acquire

apoC-II and apoE from HDL in the lymph as well as in the circulatory system. Later, chylomicrons transfer apoA-I and apoA-IV (in rats) or apoA-II (in humans) back to HDL before they are degraded into chylomicron remnants by lipoprotein lipase (LpL). LpL enzymes are located on capillary endothelial cell surfaces and they facilitate release of the free fatty acids which are taken up by muscle and adipose tissue. Since apoC-II is a required co-factor for LpL, it is not transferred back to HDL until the chylomicron has completed its task of delivering TGs, apoC-II. Remnants are then taken up by LDL receptors and LDL receptor related proteins (LRP) on liver parenchymal cells (Vance and Adeli, 2008). The high concentration of TG loaded lipoprotein in the postprandial state is by in large comprised of chylomicrons, which accounts for 80% of the postprandial increase in TG levels (Adiels et al., 2008; Green and Glickman, 1981; Havel et al., 1987).

Forward lipid transport describes the process by which lipids are distributed to body tissues via lipoprotein molecules produced by the liver and intestine. These lipoproteins contain high amounts of TG and a single molecule of apoB. In humans, the liver produces the entire apoB100 while intestinal enterocytes produce the shortened apoB-48 by an mRNA editing mechanism. Rodent livers on the other hand secrete apoB100 as well as apoB48. Within the plasma, cholesterol ester transfer protein (CETP) transfers CE from HDL and LDL to nascent VLDL in exchange for TG to generate mature VLDLs. HDLs also provide various other apolipoproteins such as apoE and apoC-II that are transferred onto VLDL. Hepatic lipase and LpL are responsible for converting VLDL into IDL and subsequently LDL as they hydrolyze TG into free fatty acids. While most of the VLDL remnants go on to become LDL, some of the circulating VLDL remnants along with LDL are

taken up by both the LDL receptors and the scavenger receptor B-I (SRB-I) primarily in the liver (Vance and Adeli, 2008).

Reverse cholesterol transport describes the process of relying on HDL to carry cholesterol from bodily tissues to the liver for excretion. Cholesterol can be effluxed from macrophages by several different pathways. The ATP binding cassette A1 transporter (ABCA1) on macrophages has the ability to unidirectionally transfer cholesterol to lipid-free apoA-I producing nascent HDL. Nascent HDL containing free cholesterol is processed by LCAT, resulting in mature HDLs containing CE (Rader et al., 2009). The ATP binding cassette G1 (ABCG1) on macrophages can then facilitate the transfer of additional free cholesterol into mature HDL. Mature HDL can transport the CE back to the liver for selective uptake mediated by the scavenger receptor SR- BI with its subsequent biliary excretion. Alternatively, CE can be transferred by CETP to VLDL and LDL. VLDLs and LDLs carrying CE can be taken up by the liver by the LDL receptor (LDLR) (Rader et al., 2009).

1.3. Atherosclerosis

1.3.1. Atherosclerosis development through foam cell formation

Atherosclerosis is the development and accumulation of lipid molecules within the arterial wall and this occurs in several stages. In the beginning stages subendothelial lipoproteins accumulate, often at branch points of the arterial tree where the flow is disrupted. Various biological responses occur including inflammatory responses whereby

cholesterol accumulates in subendothelial macrophages (Tabas, 2002). Circulating lipoproteins cross into the intima in response to this accumulation of lipoproteins and monocytes that are recruited to this area (Takahashi et al., 2002). Monocyte chemoattractant protein-1 (MCP-1) is a key facilitator in recruiting monocytes into the atherosclerotic lesions. These monocytes differentiate and proliferate into macrophages when stimulated by macrophage colony-stimulating factor. The macrophages then begin engulfing the modified lipoproteins with the scavenger receptor on these macrophages being primarily responsible. The predominant modified lipoprotein is oxidized LDL. Due to their appearance under the microscope, these macrophages which are engorged with CE droplets have been termed foam cells (Takahashi et al., 2002).

1.3.2. Inflammation

Particular tissues of an organism can be in a state of inflammation as a response to either internal or external stress factors. This can arise from activating the tissue or the organism's host defence to respond to any object deemed foreign and dangerous to the organism. The inflammatory response, as a part of the immune response, is comprised of a complex network of intricately linked pathways that are not yet completely understood. It has been commonly observed that atherosclerotic lesions are heavily laden with immune cells, paving the way for inflammation to be the underlying mechanism of atherosclerosis development. There are three levels of mechanisms involved in inflammatory responses and these mechanisms are classified being either as cell-specific, signal-specific, or gene-specific (Medzhitov and Horng, 2009). The internalization and retention of cholesterol in

macrophages is amplified during inflammation since pro-inflammatory cytokines play a major role in preventing cholesterol efflux. This is accomplished by inhibiting the expression of ABCA1 and ABCG1 which causes the macrophage to become a foam cell (Hansson et al., 2006).

Figure 1.1 Progression of atherosclerosis

This diagram depicts the progression of atherosclerosis development with LDL accumulation in the fatty streak in a) followed by an intermediate lesion in b), which later develops into a more advanced lesion that is able to rupture in c) and an advanced stage lesion that will occlude blood flow. Adapted from (Rader and Daugherty, 2008).

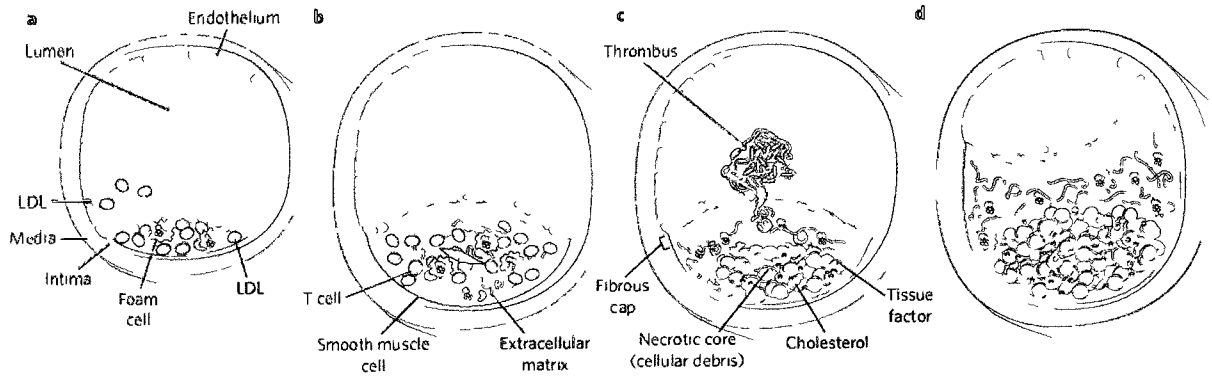
a
Endothelium
Lumen
LDL
Media
Intima
Foam cell
LDL
b
T cell
Smooth muscle cell
Extracellular matrix
c
Thrombus
Fibrous cap
Necrotic core (cellular debris)
Cholesterol
Tissue factor
d

1.4. Cardiovascular disease and oral health deficiency

1.4.1. Is there a link between microbial pathogens and CVD?

More than 100 years ago there was an initial proposal by Osler that infections were a risk factor for CVD. However nobody pursued it any further until the 1970s when it was shown that Marek's disease virus of the herpes virus family can cause atherosclerosis in chickens, regardless of the levels of cholesterol (Fabricant et al., 1978). Soon after that, many studies began appearing, showing that a variety of infections, both chronic and acute, brought on by viruses as well as bacteria could contribute to the development of atherosclerosis (Mattila et al., 2005). However, the underlying connection between infection and CVD has been difficult to uncover.

1.4.2. Periodontal disease and its risk factors

According to the National Institute of Dental and Craniofacial Research, approximately 80% of Americans have some form of gum disease, ranging from mild inflammation of the gums to more severe stages. Early stages of gum disease are termed gingivitis, where there is inflammation of the gum tissue. The later stage of gum disease, manifested by serious damage to any combination of the gums, teeth and supporting bones, is called periodontitis. Any individual diagnosed with periodontitis would most certainly require professional dental assistance (National Institutes of Health, 2010).

Periodontal disease can be classified into two categories, less severe gingivitis and the more severe periodontitis. Poor oral health will attribute to increase the pathogen burden and subsequently increased disease. Several epidemiological studies have shown that periodontal disease is positively correlated with atherosclerosis. In the Oral Infections and Vascular Disease Epidemiology Study (INVEST), Desvarieux *et al.* found a significant association between the number of teeth lost, as a marker for past periodontal disease, and carotid artery plaque (Desvarieux et al., 2003) and between microbial burden in the oral cavity and carotid artery plaque (Desvarieux et al., 2005). Recently, individuals with past incidences of coronary heart disease have been found to carry significant titres of specifically *Porphyromonas gingivalis* antibodies amongst 12 different pathogen antibodies tested (Yamazaki et al., 2007). This link between periodontitis and cardiovascular disease is definitely gaining traction. It has now caught the attention of the editorial boards of both the American Journal of Cardiology and the Journal of Periodontology and they came together to publish an editor's consensus to address this recently (Friedewald et al., 2009).

1.5. *Porphyromonas gingivalis* in cardiovascular disease

A study at the Ohio State University College of Dentistry found that the prevalence of *Porphyromonas gingivalis* was detected significantly higher in people with periodontitis (79%) compared to healthy controls (25%) (Griffen et al., 1998). *P. gingivalis* belongs to a family of anaerobic bacteria previously classified as Bacteroides. It is a gram negative rod shaped bacteria that is found in the oral cavity. It carries several virulence factors such as

fimA, LPS and proteinases (gingipains). Many studies have shown the presence of *P. gingivalis* in atherosclerotic plaque however, it was not known whether the bacteria were already inactivated until recently. In addition to performing quantitative PCR (QPCR) indicating that the bacterium *P. gingivalis* was present in human atherosclerotic plaque, Kozarov et al., has been able to take it a step further and show that the *P. gingivalis* was indeed viable using a cell invasion assay (Kozarov et al., 2005). Since *P. gingivalis* has been strongly associated with periodontitis, Dorn and colleagues tested the ability of 3 different periodontal pathogens (*Eikenella corrodens, Porphyromonas gingivalis,* and *Prevotella intermedia*) to invade human cells (endothelial & smooth muscle) and they found that *P. gingivalis* can indeed invade human coronary artery cells (Dorn et al., 1999). They followed this up by testing 26 different strains of *P. gingivalis* and found a total of 25 of 26 strains tested were able to be internalized. Most of these were moderately invasive as only 4 strains were highly invasive with strain #381 being the most invasive (Dorn et al., 2000).

1.5.1. A role for *P. gingivalis* in cardiovascular disease in mice

Mice have been the model most extensively used for establishing the association between periodontitis and atherosclerosis. Li et al used 10 week old male, apolipoprotein E (apoE) +/- mice, split into 2 diet groups: regular chow and high fat diet. These mice were infected intravenously with 10^7 CFU of *P. gingivalis* once per week (Li et al., 2002). The mice were sacrificed at either 10, 14 or 24 weeks after infection (Li et al., 2002). Results showed that *P. gingivalis* infection indeed accelerated atherosclerosis progression (Li et al., 2002). Aortic atherosclerotic lesions developed earlier, were larger and more advanced

than those in the controls not infected with *P. gingivalis* (Li et al., 2002). Li et al. suggest that infection alone is not the sole cause of atherosclerosis but rather an accelerator (Li et al., 2002). Gibson et al have shown through oral inoculations that only an invasive strain of *P. gingivalis*, was able to promote atherosclerosis in apoE-deficient mice via a specific method of activating TLRs (Gibson et al., 2004). It was also suggested that immunization against *P. gingivalis* can reduce the risk of accelerated atherosclerosis due to infection (Gibson et al., 2004). Lalla et al. infected apoE-deficient mice both orally and anally with *P. gingivalis* and found increased atherosclerotic plaques compared to non-infected controls (Lalla et al., 2003). The difference in lesion area within the aortic sinus was, on average, 40%. Mice infected with *P. gingivalis* showed significantly increased alveolar bone loss. A positive correlation between alveolar bone loss and atherosclerotic lesion area was recorded (Lalla et al., 2003).

It has been shown previously in the Whitman laboratory that *P. gingivalis* requires caspase-1 to activate the proinflammatory mechanism that is responsible for infection-accelerated atherosclerosis (Gage et al., unpublished results). Following oral infection, alveolar bone loss in caspase-1 competent apoE -/- mice was found to be significantly more (25% and 34% in males and females, respectively) than that in non-inoculated littermates with an identical genotype (Gage et al., unpublished results). There was an unexpected finding that alveolar bone loss was further reduced in non-inoculated caspase-1 deficient mice compared to that in the caspase-1 competent mice (43% in males and 47% in females) (Gage et al., unpublished results). Atherosclerotic lesion development was

accelerated in inoculated caspase-1 competent mice (by 105% in males and 60% in females) compared to their non-inoculated control littermates that were caspase-1 competent (Gage et al., unpublished results). These non-inoculated littermates showed no difference in atherosclerotic lesion sizes to caspase-1 deficient mice both with and without any *P. gingivalis* inoculation (Gage et al., unpublished results).

1.6. Interleukin-1β biochemistry & regulation

1.6.1. IL-1β structure

IL-1β is a well known extracellular pro-inflammatory cytokine that is commonly released when called upon during inflammation. In humans, it is produced primarily by monocytes, macrophages, keratinocytes and Langerhans cells. IL-1β has many similarities and differences to another member of the IL-1 family: IL-1α. Both have their structure defined by β-sheets. Both are translated in the cytosol and are not translocated into the endoplasmic reticulum (ER) (Dinarello, 1996) as they lack a classical signal sequence. However, unlike IL-1α, IL-1β is secreted. Another difference is that IL-1β has an unmistakable TATA box within its promoter region while IL-1α does not (Dinarello, 1996) suggesting that IL-1β is more readily transcribed than IL-1α. Over the years, the structure of IL-1β has been resolved to a greater degree. In the late 1980's Priestle et al. refined the crystallography model of IL-1β to 3Å and subsequently 2Å. IL-1β is composed of 12 anti-parallel β-strands folded into the shape of a tetrahedron (Priestle et al., 1989). Two anti-parallel β-strands form hydrogen bonds along each of the edges of the tetrahedron as the

hydrophobic side chains point towards the inside of the tetrahedron. A six-stranded anti-parallel β-barrel occurs at one of the vertices. Currently, optimal elucidation of protein structure requires x-ray crystallography in conjunction with NMR (Floudas, 2007). However, computer modeling is becoming increasingly accurate in the predicting of protein structure, in particular three-dimensional spatial configuration. The crystal structure of IL-1β complexed with IL-1 Receptor Type 1 (IL-1R1) has been elucidated in the late 1990's (Vigers et al., 1997). IL-1R1 is a rare receptor in which IL-1β can bind and subsequently magnify its own production of IL-1β. Nature has cleverly designed an antagonist in the IL-1R2, which is a decoy receptor that binds IL-1β and mutes it. The human IL-1β 3D rendered structure based on X-ray crystallography with NMR refinement can be seen in figure 1.2.

1.6.2. IL-1β regulation

There is a class of transmembrane proteins on immune cells called toll-like receptors (TLRs). TLRs belong to group of proteins called pattern recognition receptors (PRR) which are able to recognize common structural motifs. Activating the appropriate TLRs stimulates transcription and translation of IL-1β. Pathogen-associated molecular patterns (PAMPs) are proinflammatory mediators that bring about increased expression of inflammatory cytokines such as IL-1β, IL-6 and TNF-α. Lipopolysaccharide (LPS) is the main component of gram-negative bacteria cell walls which activates multiple macrophage functions responsible for host immune and inflammatory responses. LPS is often used in experiments as a mediator to stimulate a proinflammatory response in macrophages. Alongside TLRs, IL-1 receptors (IL-1R) are structurally similar to PRRs and can also recognize

various PAMPs in addition to IL-1β. Type 1 IL-1R (IL-1R1) is required for recruiting adaptor molecules such as MyD88, and activating IL-1R-associated kinases (IRAK). This activates nuclear factor –κB (NF-κB) and mitogen-activated protein kinase (MAPK)-regulated transcription factors (c-jun n-terminal kinase (JNK) and p38). NF-κB is key to the transcriptional regulation of IL-1β (Barksby et al., 2007). An abundance of studies have demonstrated that LPS activates the proinflammatory response via TLR4, found on plasma membrane rafts. However, these studies have been performed using LPS that is commercially available and this LPS is extracted and purified from *Escherichia coli*. Recently, LPS extracted from *P. gingivalis* has shown some novel results. Instead of strictly adhering to interacting and signaling through TLR4, *P. gingivalis* LPS has been shown to activate the proinflammatory response via TLR2, both in vitro and in vivo (Burns et al., 2006; Zhang et al., 2008). This has been an interesting finding since it has been understood that gram-positive bacteria generally signal through TLR2, while gram negative bacteria signal through TLR4. Yet *P. gingivalis* is gram negative. *P. gingivalis* has been shown to be able to activate TLR2 and TLR4 independently, based on different purified cell wall components (Zhou and Amar, 2007). Human vascular endothelial cells in culture normally express TLR4, but TLR2 and 4 are ramped up upon proinflammatory cytokine stimulation (Reiss and Glass, 2006). This magnification of TLR2 expression upon stimulation of proinflammatory cytokines can provide the basis for a chronic inflammation condition.

The activated monocyte/macrophage releases ATP into the extracellular space. ATP activates the P2X7 receptor (P2X7R) which causes an immediate K^+ efflux from the cell. This

allows the caspase-1 inflammasome to assemble. The assembled caspase-1 inflammasome initiates the processing of pro-caspase-1 which produces the active caspase-1. Active caspase-1 in turn processes the pro-IL-1β into the active IL-1β by cleaving the 33.1 kDa precursor pro-IL-1β into the mature 17.5kDa. This cleavage process occurs between Asp116 and Ala117 (Tardif et al., 2004) and can happen either in the cytosol or in secretory lysosomes, which can be then released from the cell (Dinarello, 2009). Because of this function, caspase-1 is also known as IL-1β -converting enzyme (ICE). The relatively inactive pro-IL-1β stays in the cytosol until it is cleaved and then it is moved out of the cell (Dinarello, 1997). Recently, another non-classical secretory pathway for IL-1β has been shown to require the P2X7R-induced release of exosomes-containing IL-1β, caspase-1 and inflammasome components, within microvesicles (Qu et al., 2007).

The IL-1β promoter is unique as it has regulatory regions ranging from thousands of base pairs upstream to a few base pairs downstream of the transcriptional start site. Two independent enhancer regions are present which act cooperatively with each other. The consensus is that gene expression of IL-1β is regulated at various levels. Dependent on the stimulant, the concentration of IL-1β mRNA can intensify within 15 min. Various stimuli will maintain high levels of IL-1β mRNA for varying lengths of time but mRNA levels can start to fall at 4 hours. This decrease could be attributed to transcriptional repressor synthesis and / or reduced mRNA half-life (Dinarello, 1996). However when IL-1β is used to stimulate its own gene expression, its mRNA levels can be maintained for more than 24 hrs at a time. IL-1β gene expression and protein synthesis in monocytes with histamine can be

boosted by raising cAMP levels. Retinoic acid has the ability to stimulate IL-1β mRNA production but these primary transcripts do not yield mature mRNA. Oddly enough, when cycloheximide is added to interfere with translation, exon splicing and intron excision of immature IL-1β mRNA into mature mRNA is increased. This process, classified as superinduction, involves an activation step to get around the intrinsic inhibition before the precursor mRNA can be processed (Dinarello, 1997). Only IL-1β and TNFα exhibit a segregation of activity between transcription and translation. Most of the IL-1β mRNA is in fact degraded and minimal translation into pro-IL-1β occurs. Increased translation can be induced by two ways: by adding IL-1 to cells with high levels of IL-1β mRNA and by removing cycloheximide after superinduction. It has been proposed that stabilization of the AU rich 3' untranslated region occurs in cells that are stimulated by LPS. These AU-rich sequences have been shown to suppress normal hemoglobin synthesis. Stabilization of mRNA with LPS explains how low concentrations of LPS per cell can generate a higher concentration of translated IL-1β. It has also been explained that IL-1 stabilizes its own mRNA via deadenylation prevention. This is something that occurs for the chemokine gro-χ. Removing IL-1 from cells after a 2 hour incubation causes the poly(A) to shorten. IL-1 thus seems to be important in the regulation of gro synthesis. The cytokines that IL-1 stimulates, respond to low concentrations of IL-1 while producing high levels of chemokines. As an example, 1pM of IL-1 can induce fibroblasts to produce 10nM of IL-8 (Dinarello, 1997).

1.6.3. Pathophysiology of IL-β

IL-1β is responsible for the stimulation of neighbouring monocytes and macrophages, recruiting assistance in the response to inflammation. Given the immediate release of IL-1β, it has the capability of being the alarm system for the body in the event of an infection. Various pathogens have been shown to have the ability to bring about increased IL-1β. For example, *Helicobacter pylori* can activate increased IL-1β and TNFα production (Portal-Celhay and Perez-Perez, 2006). Patients with *H. pylori* infections showed a solid correlation between IL-1β and IL-8 levels of expression alluding to the potential relationship between these two cytokines (Noach et al., 1994). *Salmonella* strains have been shown to up-regulate IL-1β and IL-18 by activating caspase-1, which promotes inflammation (Guiney, 2005). *Pseudomonas aeruginosa* is a gram-negative, opportunistic pathogen which affects immunocompromised people and those with malignancies. *P. aeruginosa*, like *Salmonella typhimurium* and *Shigella flexneri*, use ICE protease activating factor (IPAF) and apoptosis speck-like protein containing CARD domain (ASC) (both of which are adaptor proteins for the inflammasome complex) to regulate IL-1β and IL18 through caspase-1 (Martinon, 2007). It should be noted that with *P. aeruginosa* flagellin is generally required to activate the inflammasome pathway (Franchi et al., 2007) and it has also been shown that at least one strain does not require the flagellin. Recently, Case et al., has shown that *Legionella pneumophila*, a bacterium that required caspase-1, IPAF and bacterial flagellin but not ASC to become ill with Legionnaire's disease (Case et al., 2009). This further supports the notion that the host immune response is slightly different for different bacteria.

Figure 1.2: IL-1β visualized by x-ray crystallography and refined by NMR
Adapted from (Shaanan et al., 1992)

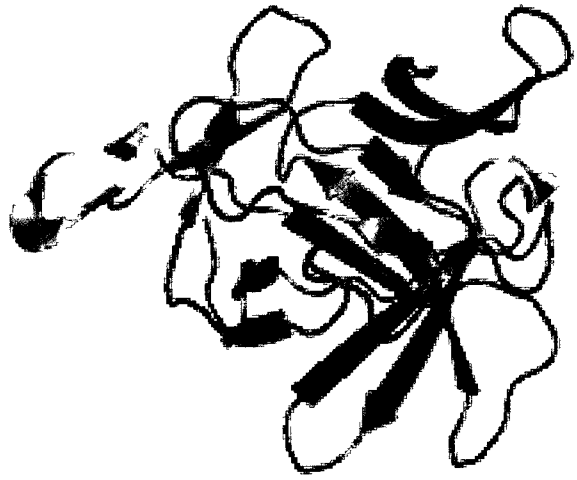

1.6.4. Potential role of IL-1β in disease, a focus on atherosclerosis

When IL-1β was knocked out in apoE-null mice, it was found that atherosclerotic lesions in the aortic root were reduced by 33% and 32% when compared to 12- and 24-week old wild type apoE-null mice respectively (Kirii et al., 2003). *P. gingivalis* has been shown to induce secretion of proinflammatory cytokines such as IL-1β *in vitro* (Bodet et al., 2006). Given that various pathogens require IL-1β for initiating and propagating inflammation, in addition to the caspase-1 findings by Gage within our lab, we propose to test the hypothesis that IL-1β is required in the development of *P. gingivalis*-accelerated atherosclerotic lesions.

1.7. Using apoE mouse model for atherosclerosis study

1.7.1. Background on apoE mouse model

With the need for an optimal in vivo model to study atherosclerosis and since mice are naturally resistant to atherosclerosis, the race began to produce a mouse that would be susceptible to atherosclerosis. Two groups concurrently produced the apolipoprotein (apo) E-null mouse with Nobuya Maeda's group from the University of North Carolina reporting first followed soon after by Jan Breslow's group at Rockefeller University (Piedrahita et al., 1992; Plump et al., 1992). Both groups employed the same method of gene targeting in mouse embryonic stem (ES) cells. The LDLR knockout mouse was created using the same technique of homologous recombination in ES cells by the world renowned Brown and Goldstein group from the University of Texas Southwestern Medical Center.

The apoE-null mice recorded high levels of chylomicron remnants, VLDLs and IDLs. LDLR-null mice on the other hand, had specifically elevated levels of LDL. ApoE deletion causes atherosclerosis in mice because without the apoE, chylomicrons cannot be cleared, resulting in a disease state similar to that of familial type 3 hyperlipoproteinemia. The LDLR deletion in mice reproduces the condition of familial hypercholesterolemia homozygotes in humans by causing atherosclerosis due to several reasons. Since IDLs are cleared via LDLRs on the liver, IDL levels rise when they cannot be cleared by a lack of LDLRs. Even though IDLs contain both apoE and apoB-100, it is apoE that binds to LDLR with high affinity and studies have shown that IDL clearance is apoE dependent (Ishibashi et al., 1994).

Clearing chylomicron remnants is apoE dependent. Chylomicrons contain apoB-48, which cannot bind with the LDLR. Normally, the apoE on chylomicrons generally dock onto LDLRs for clearance. However, if the LDLR is non-functional or knocked out, as in familial hypercholesterolemia homozygotes, chylomicron levels should be increased, but this is not seen. This phenomenon is explained by the existence of a backup system: the LDLR-related protein (LRP) which can bind remnants containing apoE for clearance (Ishibashi et al., 1994). One major difference between humans and mice that should be noted is that 70% of VLDLs from the murine liver carry apoB-48 as opposed to apoB-100. As a result, mouse VLDLs are not converted into LDLs as they are broken down into remnants much like chylomicrons (Ishibashi et al., 1994).

The Brown and Goldstein group crossbred apoE knockout mice with LDLR knockout mice to produce apoE & LDLR double knockout mice (Ishibashi et al., 1994). They found that the double knockout mice did not have any increased hypercholesterolemia compared to mice with just apoE knocked out. These results are consistent with other studies covering lipoprotein-receptor interactions (Ishibashi et al., 1994). In apoE-null mice, atherosclerotic lesions of type 1 through V can be found. Early lesions composed of lipid-laden foam cells as well as late lesions consisting of a necrotic core and fibrous caps can be seen in the aorta and the aortic root (Whitman, 2004). In LDLR-null mice, type 1 through IV atherosclerotic lesions can be seen in the aorta and the aortic root, ranging from mostly lipid-laden foam cells to necrotic core lesions and fibrous caps (Whitman, 2004).

There are several reasons why using mice as a model for studying atherosclerosis is advantageous, 1. There is a vast amount of genetic data pertaining to various inbred strains which has aided in the genetic links to atherosclerosis (Whitman, 2004). An N value of statistical significance can easily be obtained as mice are small in size, reproduction rate of mice is relatively fast and cost of housing mice is relatively minimal (Whitman, 2004). Mice require smaller dosages of pharmacological agents that may be costly or limited in its availability (Whitman, 2004). Specifically, using apoE or LDLR knockout mice has several advantages (Whitman, 2004). A commercial lab such as Jackson Labs has a large stock of these mice that have already been backcrossed more than 10 times onto the C57BL/6 strain and thus can be ordered on demand (Whitman, 2004). These mice breed well and produce decent sized litters, averaging 6-8 apoE pups and 4-6 LDLR pups (Whitman, 2004).

Lesion types are well documented for various ages of the mice following the American Heart Association's definition of atherosclerosis stages in humans (Whitman, 2004).

2. Rationale, Hypotheses and Specific Aims

2.1 Rationale:

It has been previously shown in our laboratory that oral inoculation of apoE -/- mice with *P. gingivalis* increased alveolar bone loss and accelerated the development of aortic sinus atherosclerosis. However, *P. gingivalis*-induced bone loss and accelerated atherosclerosis were not seen if the apoE -/- mice were also deficient in caspase 1 which indicates that caspase-1 activity is required for the pathogenic response to oral *P. gingivalis* infection. IL-1β is a substrate for caspase-1 and has been shown to participate in atherogenesis in apoE-/- mice. As a sequence of events that leads to *P. gingivalis*-accelerated atherosclerosis, we propose, that *P. gingivalis* reacts with TLRs on macrophages to activate caspase-1 which cleaves immature pro-IL-1β into the mature form of IL-1β. Mature IL-1β is released which brings about increased inflammation and consequently increased atherosclerosis. A schematic of this process is presented in figure 2.1.

2.2 Hypothesis:

i) IL-1β is a necessary inflammatory cytokine to facilitate *P. gingivalis*-mediated alveolar bone loss in both genders of apoE-/- mice.

ii) Given oral inoculations of *P gingivalis*, apoE-/- mice deficient in IL-1β will show less atherosclerotic lesions than their IL-1β competent littermates.

2.3 Project aims:

i) We will determine if the proinflammatory cytokine IL-1β is required for alveolar bone loss *in vivo*.

ii) We will determine if the proinflammatory cytokine IL-1β is required in the development of atherosclerosis following an oral *P. gingivalis* infection *in vivo*.

Figure 2.1: Rationale schematic
Depicting how *P. gingivalis* is thought to signal through TLRs, which activates caspase-1, and then processes immature pro-IL-1β into mature IL-1β that is excreted to increase inflammation and atherosclerosis

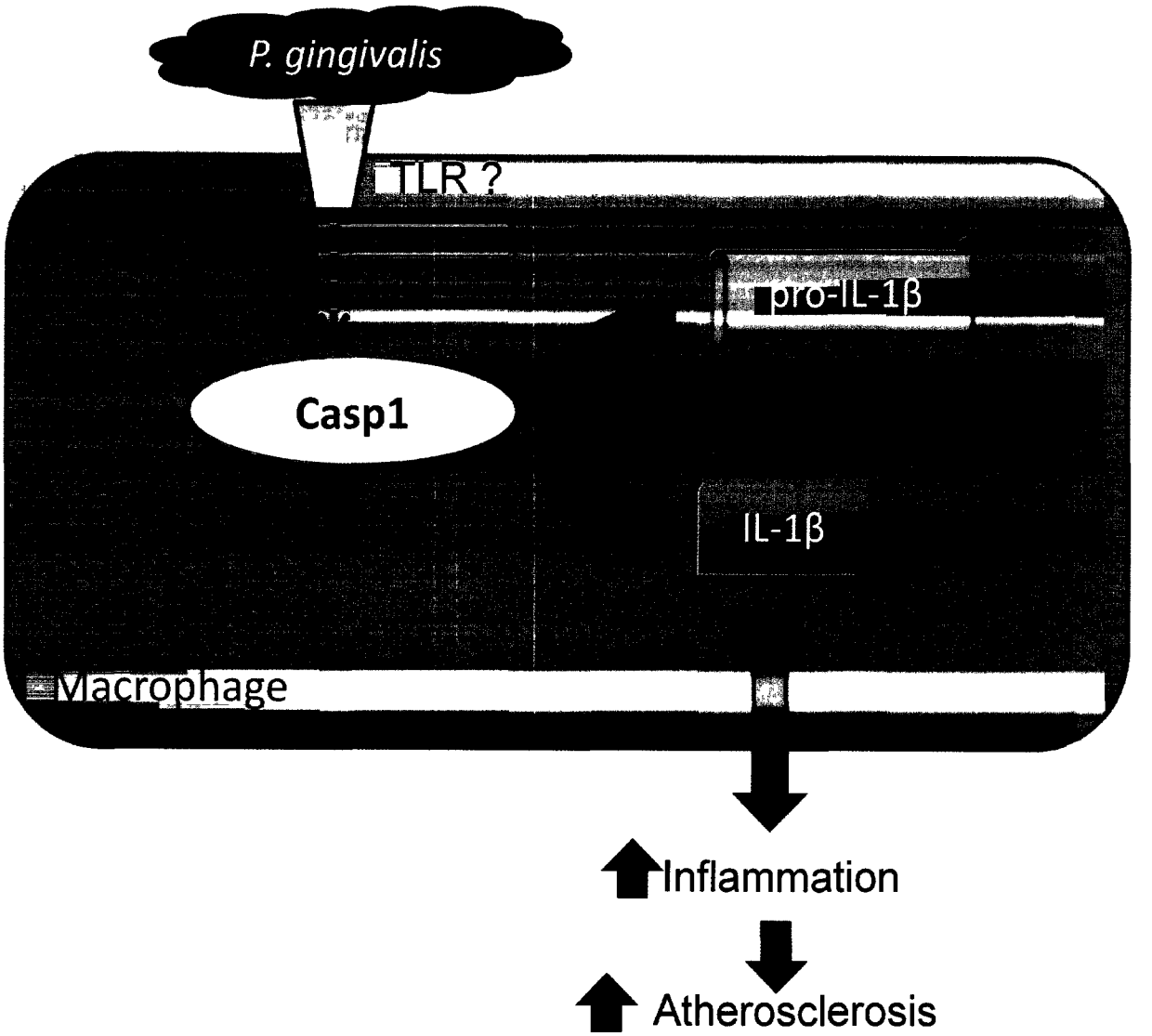
P. gingivalis
TLR ?
pro-IL-1β
Casp1
IL-1β
Macrophage
Inflammation
Atherosclerosis

3. Materials & Methods

3.1 Mice

All experimental methods requiring mice as well as the breeding of mice carried out were approved by the Animal Care Committee of the University of Ottawa. Interleukin 1-beta knockout (IL-1β -/-) mice were obtained from Dr. Mitsuru Seishima, of Gifu University School of Medicine, Gifu, Japan. The IL-1β knockout mouse was crossed onto the ApoE -/- background and this IL-1β X ApoE -/- mouse colony was kept in the conventional animal housing facilities at the University of Ottawa Heart Institute under the care of the University of Ottawa Animal Care and Veterinary Services. All breeding and experimental mice were fed regular chow diet. IL-1β competent (+/+) and knockout (-/-) littermate study mice were generated by arranging sibling breeding pairs of IL-1β +/- X ApoE -/- mice that were at least eight weeks of age. Newly born mice were weaned and genotyped at three weeks of age. Genotypes were obtained by employing polymerase chain reaction (PCR) using the following three primers: IL-1β common (5'CACATATCCAGCACTCTGCTTTCAG3'); IL-1βWT (5'GGTCAGTGTGTGGGTTGCCTTATC3') and LacZ-Kp (5'GAGGTGCTTTCTGGTCTTCACC3') (Horai et al., 1998) to elongate 720bp of IL-1β and IL-1β common 560bp of the LacZ gene. The PCR protocol consisted of 2 minutes of melting at 94°C followed by 30 cycles of melting at 94°C for 20 seconds, primer annealing at 64°C for 30 seconds and elongation at 72°C for 50 seconds. A final 10 minutes of elongation was added at the end. PCR products were separated by electrophoresis on a 1.5% agarose gel at 100V, 400mA for 26 minutes in 1X TBE buffer. A 100bp ladder (New England Biolabs)

was used to identify PCR product band sizes. Ethidium bromide-reactive fragments were visualized using a Kodak Imagestation IS440cf with a UV filter.

3.2 Inoculation of mice with *P. gingivalis*

At five weeks of age, study mice were orally given four consecutive days of 2mg/drug/day of ampicillin and kanamycin antibiotics (Sigma-Aldrich). IL-1β +/+ X ApoE -/- as well as IL-1β -/- X ApoE -/- mice (N=15) of both genders received oral bacterial inoculations of 10^{10} CFU daily inside a biohazard hood (AmCare) beginning at six weeks of age and lasted for three consecutive weeks for a total of 15 inoculations. Table 1 contains the experimental timeline and table 2 contains the classification of experimental groups. Control non-inoculated mice were handled in an identical manner as the littermates receiving inoculations. Mice were given a bolus of somnitol and sacrificed at 17 weeks of age. Calculations for an appropriate N value for each group resulted in a minimum of 14 mice, based on the requirement of attaining a power of 0.8 for a 20% change in lesion size.

3.3 Bacteria

Porphyromonas gingivalis strain 381 (alternately identified as ATCC33277) was obtained from the American Type Culture Collection (ATCC) and cultured using autoclaved MIC Anaerobe Broth (BD Biosciences) under anaerobic conditions inside an anaerobic jar with an anaerobic gas pack (Oxoid) (10% CO_2, 10% H_2, 80% N_2) at 37°C within an anaerobic chamber (Plas-Labs, Lansing MI, USA). Cultures were grown in 15ml conical tubes

(Ultident, QC, Canada) until they reached an O.D. of 0.8 at 660nm which corresponded to a concentration of 10^9 CFU/ml. Samples were centrifuged at 4000rpm, for 20 min at 30°C. Weekly PCR performed on a *P. gingivalis* sample confirmed its presence using the following primers: 5'AGGCAGCTTGCCATACTGCG3' and 5'ACTGTTAGCAACTACCGATGT3' (Operon) (Avila-Campos, 2003). To confirm purity of the *P. gingivalis* cultures, weekly samples were sent to the clinical microbiology diagnostic lab of the Ottawa Hospital, General Campus. The concentration of bacteria that the mice received was confirmed on a bi-weekly basis by plating serial dilutions of the *P. gingivalis* cultures at an OD=0.8 at 660nm on agar plates made with MIC Anaerobe Broth and agar(BD Biosciences).

3.4 Blood collection

Terminal blood samples were collected using blood collection tubes (BD Biosciences) upon puncture of the right ventricle using a 23gauge needle and a 1ml syringe. Blood was allowed 30 min to clot at room temperature followed by centrifugation at 10 000 rpm for 2 min at room temperature. Serum was stored at 4°C.

3.5 Serum cholesterol and lipoprotein profiles

Using fast protein liquid chromatography, lipoprotein profiles were generated for each group of study mice using five samples from each group. 50µl of serum was applied to a Sepharose 6 column (GE Healthcare) and 25 - 1ml fractions were collected. These fractions were analyzed following the instructions of a cholesterol assay kit (Wako

Chemical, VA) with a single modification o: the preparation and use of the 2X colour reagent rather than 1X. Total serum cholesterol was measured following the instructions of a cholesterol assay kit (DCL Genzyme Diagnostics, PEI, Canada).

Figure 3.1: A) Timeline of experimental procedure.
Every mouse undergoes this timeline, with any number of mice can be found at different stages.
Figure 3.1: B) Organization of mice by genotype and treatment.
This design was applied to each gender, resulting in 8 classification groups.

A)

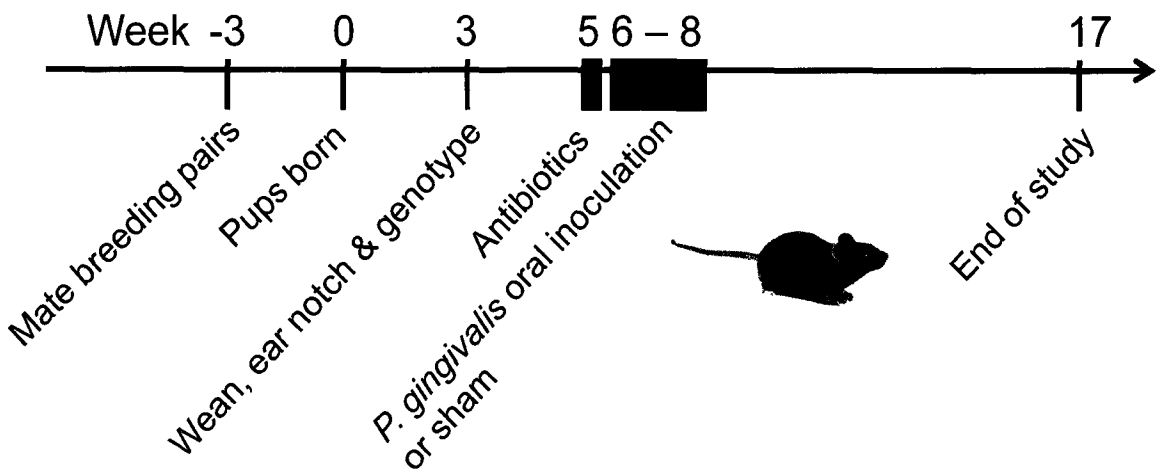

B)

	IL-1β +/+ ApoE -/-		IL-1β -/- ApoE -/-	
Control: No *P. gingivalis*	**Males N=15**	**Females N=15**	**Males N=15**	**Females N=15**
***P. gingivalis*: 5d * 3wks**	**Males N=15**	**Females N=15**	**Males N=15**	**Females N=15**

3.6 Tissue collection

Mice hearts were perfused with 1X PBS in DEPC water through a cannula inserted into the left ventricle and the perfusate was drained from a severed right atrium. Hearts were separated from the base of the aorta, embedded in optimum cutting temperature (OCT) medium (Partek/Sakura) and snap-frozen on a metal block immersed in liquid nitrogen. Hearts were then parafilm-wrapped and stored at -20°C

3.7 Quantification of alveolar bone loss

Mandibles were extracted and cleaned using surgical tools, followed by immersion in 3% hydrogen peroxide overnight. Using a Photometrics CoolSnap *cf* Pro camera (Roper Scientific Inc., Duluth, GA, USA) attached to a dissecting microscope (Nikon), digital images were taken of the lingual side of both left and right jaws laterally aligned in play-doh. The area between the cemento-enamel junction and alveolar bone crest was quantified on the lingual side by hand tracing the digital image using Image-Pro Plus software (v.6.2, Media Cybernetics, Silver Springs, MD, USA).

3.8 Quantification of atherosclerotic lesions in tissue sections

Atherosclerotic lesion sizes within the ascending aorta were determined using four serial cross sections stained with Sudan IV. Using a cryostat (Leica CM3050S) set at -18°C, sections were cut at a thickness of 10μm, 9 sections 100μm apart were collected on each of

the 10 slides. Lesion analysis commenced at the section containing the coronary ostia and disappearance of the aortic valve cusps(Daugherty and Whitman, 2003; Paigen et al., 1987). Digital photographs were taken using a Photometrics CoolSNAP *cf* camera. Using the Sudan IV stain as a guide, lesion area was determined as red-stained intimal tissue within the internal elastic lamina using Image-Pro Plus 6.2 software. The mean lesion area was obtained from four serial sections for every animal as shown in figure 3.2.

3.9 Quantification of atherosclerotic lesions in the aortic arch

Using the *en face* preparation of the aortic arch, aortas were cleaned of the body fat surrounding it, followed by cutting open the brachiocephalic artery, left common carotid artery and the left subclavian artery as well as the lesser curvature. Lastly, the aortas were pinned open on tar trays. Digital photographs were taken of the aortic arch and the area of the atherosclerotic lesion covering the vessel was quantified as a percentage of the inside area of the aorta. The area measured covered the entire aortic arch down to 3mm below the junction of the left subclavian artery and the aortic arch. No lipophylic dye was used to assist the visualization of lesions. This was adapted from (Daugherty and Whitman, 2003).

Figure 3.2: The aortic root analysis diagram

A) The anterior view of the mouse heart depicting the region of the aortic root, corresponding to the aortic sinus in **B)** A total of 9 serial cross-sections of the aortic sinus at 10μm thick, 100μm apart each were collected onto a microscope slide. **C)** An example of a sample slide of 9 sections, with the lipid stained red by SUDAN IV and nuclei counterstained with haematoxylin in blue is shown. Level 0 is determined by the disappearance of the aortic valve cusps (black arrows) and appearance of the coronary ostia (indicated by the orange arrows) as indicated by the Roman numeral i). The atherosclerosis stained red at four sections of levels 0, 100μm, 200μm & 300μm corresponding to i), ii), iii), & iv) are quantified, recorded & averaged.

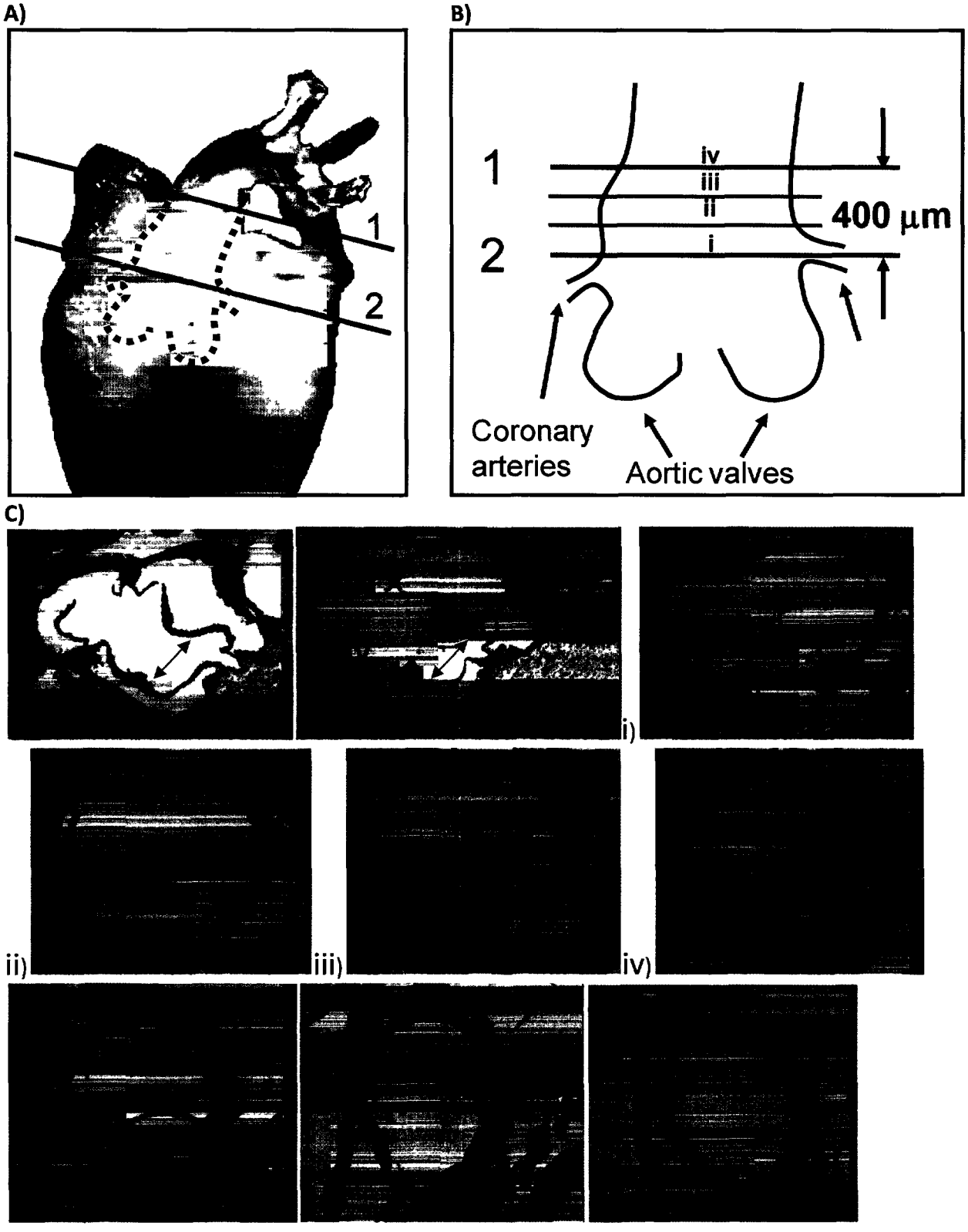
A)
1
2
B)
1
2
iv
iii
ii
i
400 µm
Coronary arteries
Aortic valves
C)
i)
ii)
iii)
iv)

3.10 Detecting serum antibodies

P. gingivalis were spun down in a microcentrifuge tube, washed twice, and resuspended in 1 ml PBS. The protein concentration of the bacterial suspension was measured by the Markwell-Lowry protein detection method. Immulon II wells were coated with 50 µl of the bacterial suspension at a concentration of 5 µg/ml and left overnight at room temperature in a wet box. The plate was washed 3 times with PBS containing 0.05% Tween 20 (PBS/Tween) followed by a saturation step with 1% BSA/PBS for one hour in a wet box. Serial dilutions of serum (stored at -20°C) were prepared in 1% BSA starting at 1:10 dilution. After removal of the 1% BSA from the antigen-coated plates, 50 µl of the serially diluted plasma was transferred to the plates starting at the highest dilution. The plate was then incubated overnight at room temperature in a wet box and the next morning, it was emptied and washed 3 times with PBS/Tween. 50 µl of an anti-mouse IgG-horse radish peroxidase conjugate (1/2000 in 1% BSA) was added and left for 2 hours at room temperature in a wet box. The plates were washed 3 times with PBS/Tween and 3 times with PBS before adding 50 µl of TMB substrate to each well. After 8 minutes, the optical density of the wells at a wavelength of 655nm (blue colour) was recorded using a BioTek Gen5 plate reader.

3.11 Statistical methods

A variety of statistical methods were used for various aspects of this project. In the total cholesterol analysis, one-way ANOVAs were used to compare the data collected between the IL-1β +/+ control and *P. gingivalis*-inoculated groups, IL-1β -/- control and inoculated

groups, between the non-inoculated control groups that were IL-1β +/+ and IL-1β -/- and finally, between IL-1β +/+ inoculated and IL-1β -/- inoculated groups. These one-way ANOVAs were performed separately for each gender. For the cholesterol profile, one-way ANOVA was performed on the raw data giving the peak of the VLDL fractions in an identical manner of comparison between the groups. Two-way ANOVA was employed to analyze alveolar bone loss where bone loss was the dependent variable while the genotype and infection were the sources. The level that the p-value must reach to be considered significant is $\alpha = 0.05$. To analyze en face atherosclerotic lesion data, we used a two-way ANOVA where again, $\alpha = 0.05$. A three-way ANOVA was also used to analyze the aortic root atherosclerosis with atherosclerosis being the dependent variable and gender, genotype and infection being the sources. Pairwise comparisons in a three-way ANOVA were conducted with the Bonferoni adjustment for multiple comparisons. The Bonferoni adjustment requires dividing the α by the number of pairwise comparisons (8 in this case) to give rise to the adjusted α of 0.00625. When a particular set of data regarding a particular level of atherosclerosis (such as level 0 in the female IL-1β -/- mice) appeared to be potentially statistically significant, one-way ANOVAs were performed where the $\alpha = 0.05$. To analyze the data from the ELISAs, a repeated measures analysis was used to compare, in both genders the slopes between the two *P. gingivalis* infected groups from the IL-1β sera.

4. Results

This project was designed to evaluate the participation of IL-1β in *P. gingivalis* mediated alveolar bone loss and atherosclerosis development. At 5 weeks of age, IL-1β+/+ apoE-/- and IL-1β-/- apoE-/- male and female mice were subjected to a 1-week oral antibiotic treatment to reduce the endogenous oral bacterial flora. Over the subsequent 3 weeks, experimental mice received 16 oral inoculations of *P. gingivalis*. Control non-inoculated mice were handled in an identical manner to the experimental mice. All mice were sacrificed at 17 weeks of age, the sera were collected for cholesterol analysis, the mandibles were collected for alveolar bone loss analysis, and the hearts and aortas were collected for atherosclerosis analysis. This experimental protocol is illustrated in figure 3.1.

4.1 Cholesterol Analysis

The total serum cholesterol of each mouse was analyzed with a cholesterol assay kit and as seen in figure 4.1, no differences were observed between the groups. Thus, neither IL-1β deficiency nor administration of *P. gingivalis* caused any changes in the total serum cholesterol levels.

Serum from individual mice (5-7 mice per group) was fractioned by FPLC, and fractions were analyzed with a cholesterol assay kit. The lipoprotein profiles shown in figures 4.2 demonstrate a similar distribution of cholesterol amongst the lipoprotein fractions in all the treatment and control groups with the cholesterol being found primarily in the VLDL fraction. While significant differences ($p<0.05$) in the VLDL peak of the lipoprotein profiles were observed between inoculated and non-inoculated IL-1β+/+ apoE-

/- groups in both males and females, as will be discussed in the following chapter, this may simply reflect a non-representative choice of samples that were analyzed.

Figure 4.1: Total serum cholesterol levels
in *P. gingivalis*-inoculated and control IL-1β+/+ and IL-1β-/- mice. Serum from all of the mice at the time of sacrifice was taken and total cholesterol concentrations were measured as described in Methods and Materials. Total serum cholesterol of all the A) male mice and B) female mice were analyzed and classified into four groups based on their genetic disposition and whether or not they were inoculated with *P. gingivalis*. Non-inoculated control mice are compared to their littermates, showing no difference in total serum cholesterol, regardless of whether they received inoculations or whether they are IL-1β-deficient.

A)

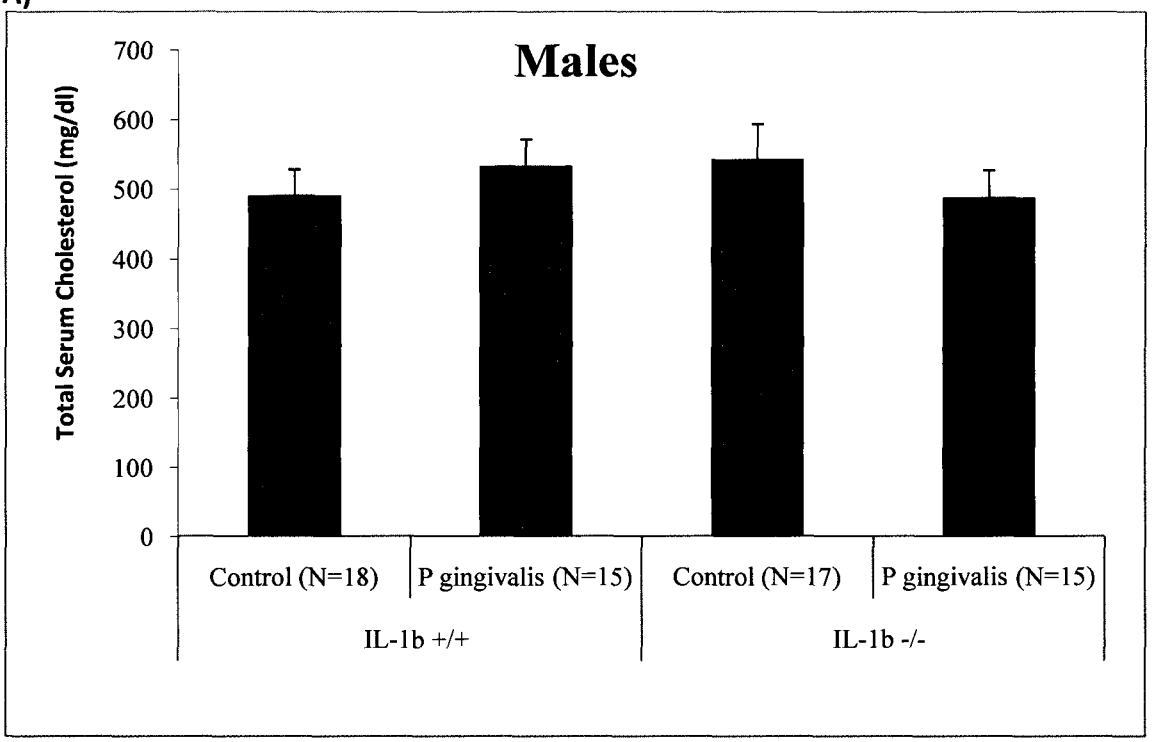
Males
Total Serum Cholesterol (mg/dl)
700
600
500
400
300
200
100
0
Control (N=18)
P gingivalis (N=15)
Control (N=17)
P gingivalis (N=15)
IL-1b +/+
IL-1b -/-

B)

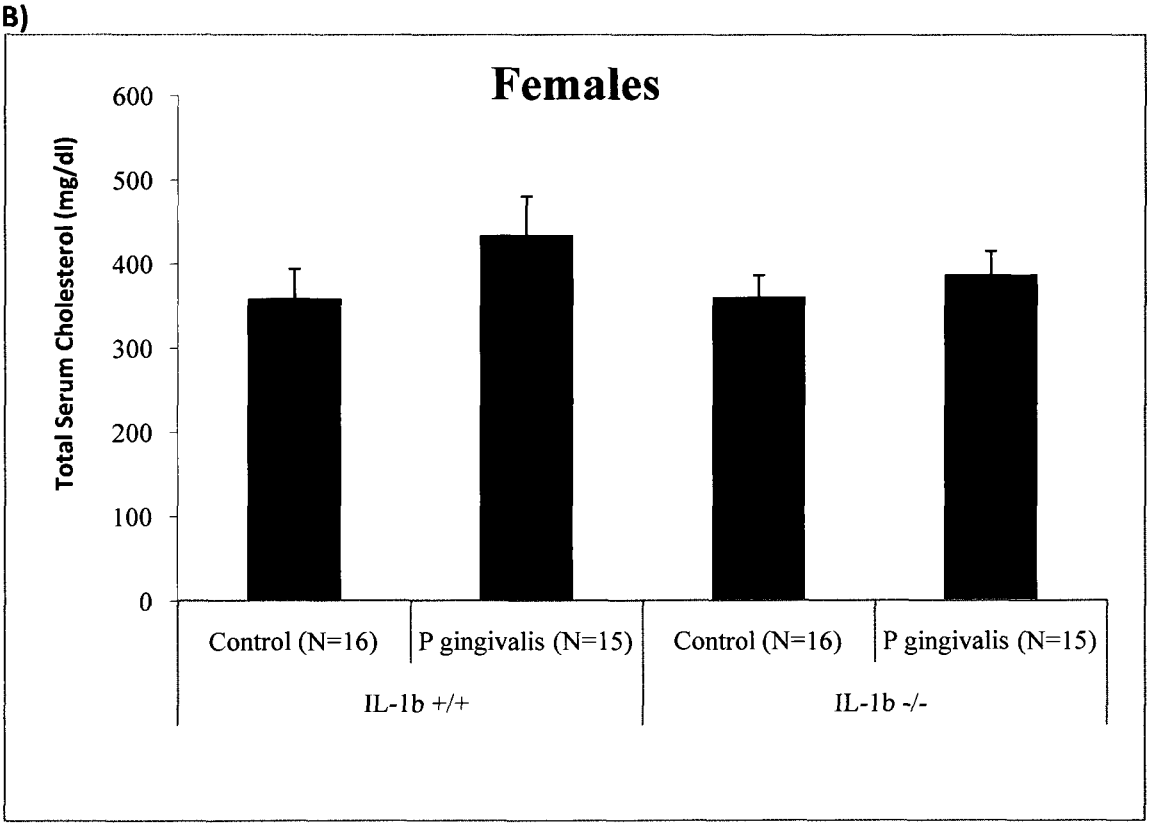
Females
Total Serum Cholesterol (mg/dl)
600
500
400
300
200
100
0
Control (N=16)
P gingivalis (N=15)
Control (N=16)
P gingivalis (N=15)
IL-1b +/+
IL-1b -/-

Figure 4.2: The distribution of cholesterol in the serum lipoprotein fractions of *P. gingivalis*-inoculated and control IL-1β+/+ and IL-1β-/- A) male and B) female mice. Serum from mice at the time of sacrifice was taken and was then subjected to FPLC chromatography as described in Methods and Materials and total cholesterol levels in the fractions were determined. Fractionated serum cholesterol of all the male mice were analyzed and classified into four groups based on their genetic disposition and whether or not they were inoculated with *P. gingivalis*. Non-inoculated control mice are compared to their littermates, showing no difference in their lipoprotein profiles, regardless of whether they received inoculations or whether they are IL-1β-deficient.

A)

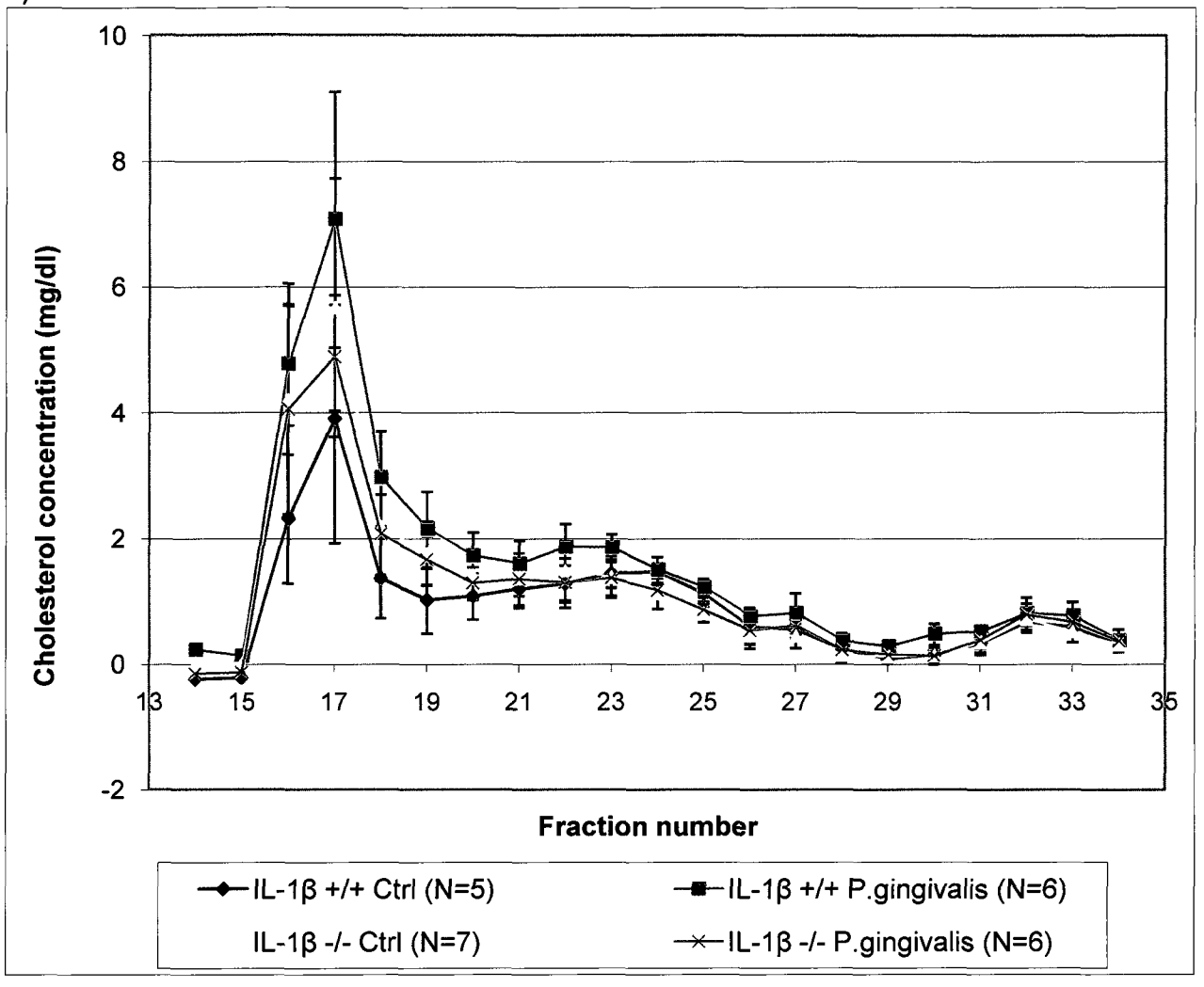
10
8
6
4
2
0
-2
13
15
17
19
21
23
25
27
29
31
33
35
Cholesterol concentration (mg/dl)
Fraction number
IL-1β +/+ Ctrl (N=5)
IL-1β +/+ P.gingivalis (N=6)
IL-1β -/- Ctrl (N=7)
IL-1β -/- P.gingivalis (N=6)

B)

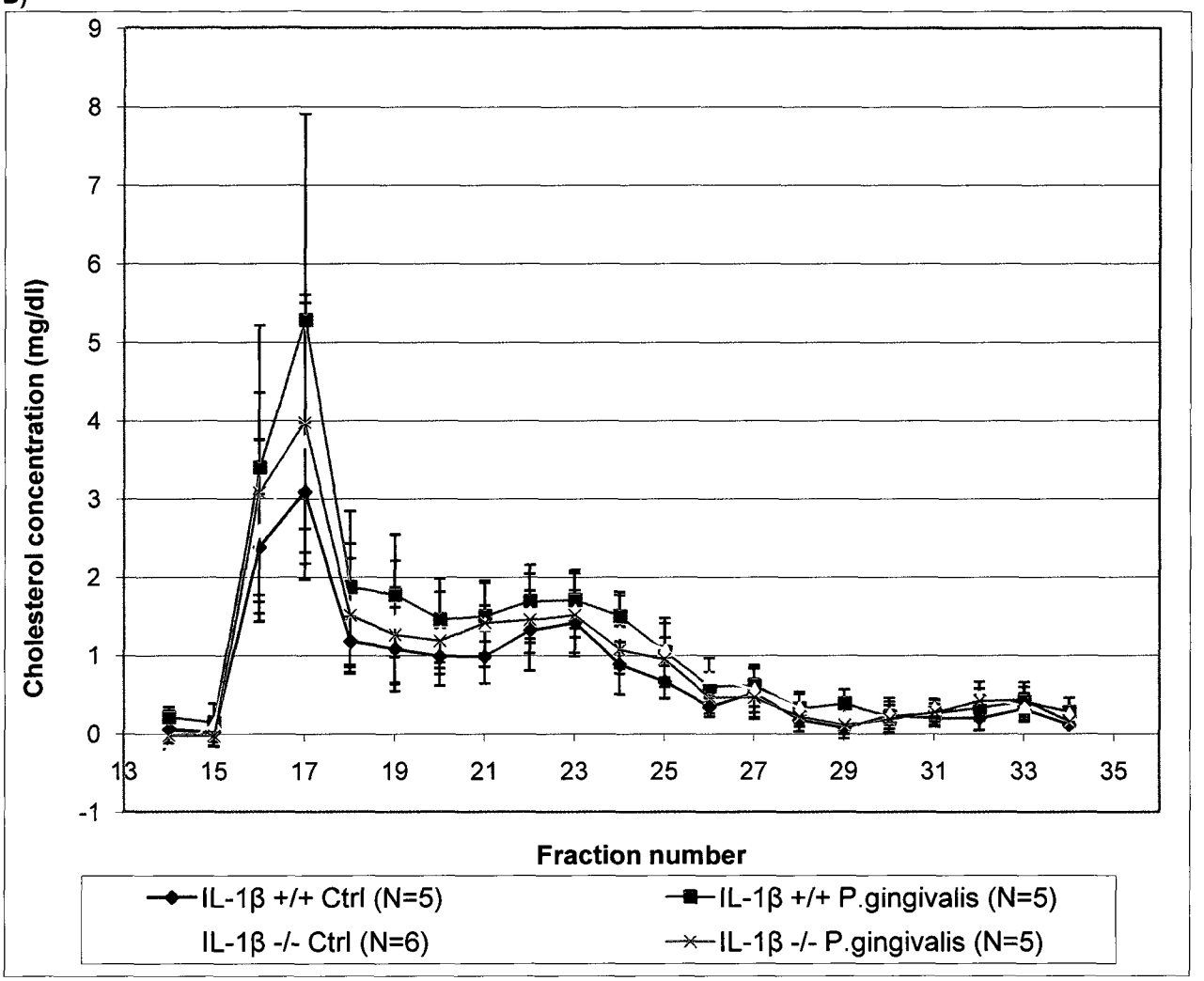
Cholesterol concentration (mg/dl)
9
8
7
6
5
4
3
2
1
0
-1
13
15
17
19
21
23
25
27
29
31
33
35
Fraction number
IL-1β +/+ Ctrl (N=5)
IL-1β +/+ P.gingivalis (N=5)
IL-1β -/- Ctrl (N=6)
IL-1β -/- P.gingivalis (N=5)

4.2 Alveolar Bone Loss

Measuring the amount of bone loss is a method used by many researchers as a tool to indicate that the mouse experienced periodontal disease to a high enough degree to produce bone regression. Mandibles of each mouse were extracted, cleaned and photographed. Bone regression was measured in mm^2 between the alveolar bone crest and cemento-enamel junction and tabulated. While the results in figure 4.3 appear to show that *P. gingivalis* had no effect on bone regression, IL-β deficiency did. Irrespective of gender and whether the mice received *P. gingivalis* inoculations, IL-1β deficiency attenuated bone loss presumably due to the inability to promote the pro-inflammatory state ($p=0.0014$, Three-way ANOVA). This effect was still seen even though the IL-1β-deficient males did demonstrate a trend towards more bone loss when infected with *P. gingivalis* compared to their non-infected IL-1β-deficient littermates.

Figure 4.3: The effect of *P. gingivalis* inoculation on alveolar bone loss in IL-1β+/+ and IL-1β-/-

A) ***male mice.*** Six-week old IL-1β+/+ *and* IL-1β-/- male mice were inoculated with *P. gingivalis* as described in Methods and Materials and mandibular bone loss was evaluated when mice were sacrificed at 17 weeks of age. *P. gingivalis* inoculation of IL-1β+/+ male mice does not increase alveolar bone loss. There is, however, significantly less bone regression in IL-1β-/- mice compared to IL-1β+/+ mice irregardless of *P. gingivalis* infection (*p=0.024, 2 way ANOVA where $p<0.05$ is significant). Inoculation of IL-1β-/- mice with *P. gingivalis* shows a trend towards increased bone loss when compared to non-inoculated IL-1β-/- *littermates.*

B) ***female mice.*** Six-week old IL-1β+/+ *and* IL-1β-/- male mice were inoculated with *P. gingivalis* as described in Methods and Materials and mandibular bone loss was evaluated when mice were sacrificed at 17 weeks of age. *P. gingivalis* inoculation of IL-1β+/+ female mice does not increase alveolar bone loss. There is, however, significantly less bone regression in IL-1β-/- female mice compared to IL-1β+/+ female mice irregardless of *P. gingivalis* infection (◊p=0.0266, using 2 way ANOVA where $p<0.05$ is significant).

A)

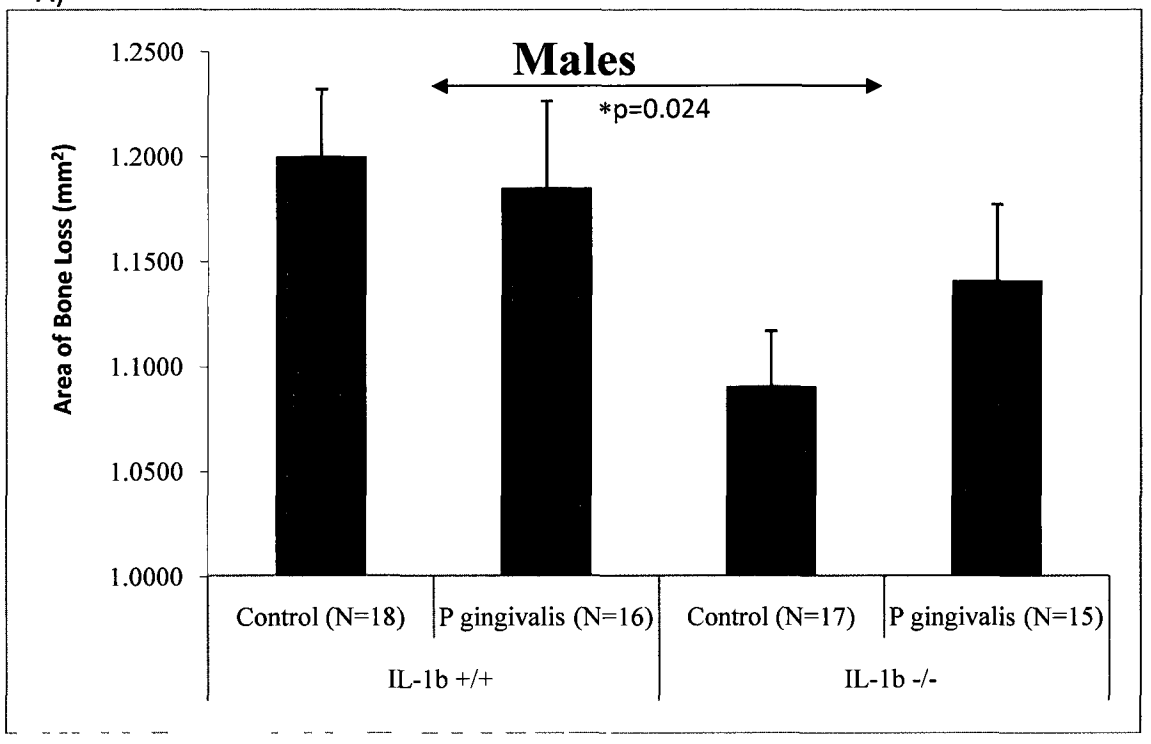
Males
*p=0.024
Area of Bone Loss (mm²)
1.2500
1.2000
1.1500
1.1000
1.0500
1.0000
Control (N=18)
P gingivalis (N=16)
Control (N=17)
P gingivalis (N=15)
IL-1b +/+
IL-1b -/-

B)

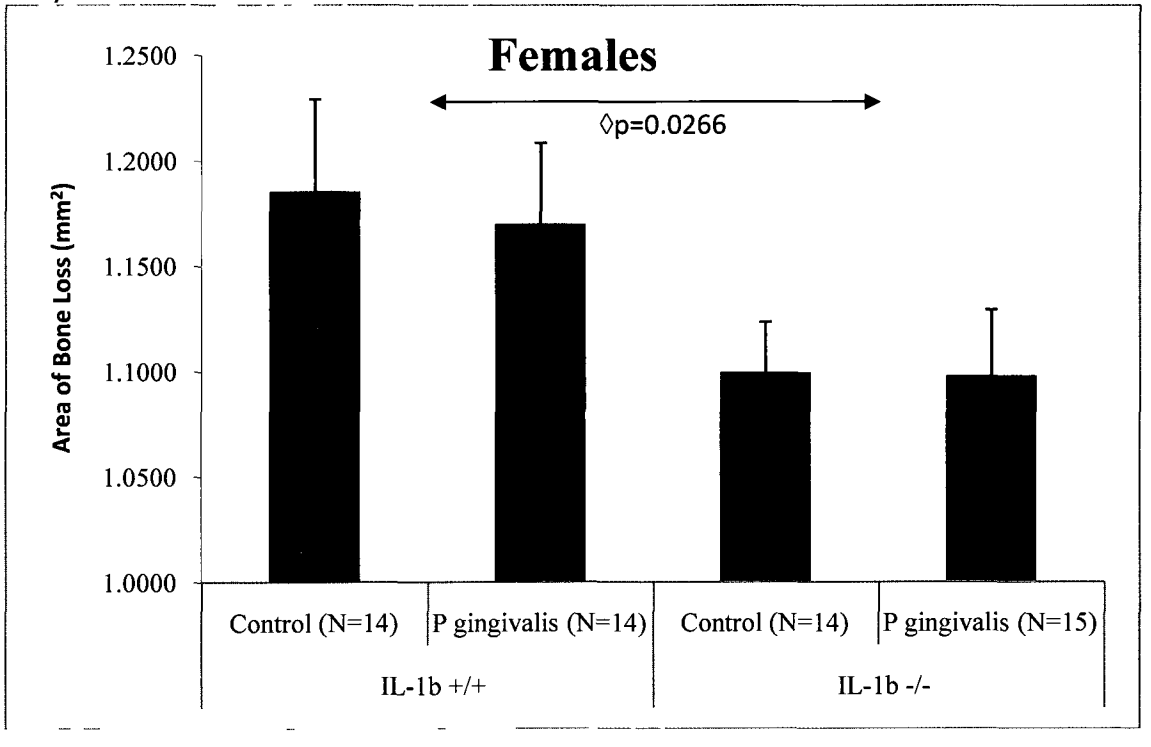
Females
◊p=0.0266
Area of Bone Loss (mm²)
1.2500
1.2000
1.1500
1.1000
1.0500
1.0000
Control (N=14)
P gingivalis (N=14)
Control (N=14)
P gingivalis (N=15)
IL-1b +/+
IL-1b -/-

4.3 Atherosclerosis Analysis

4.3.1 *En face* atherosclerosis analysis

The *en face* method of analyzing atherosclerosis involved severing the aortic arch from the aortic root inside the heart and at the thoracic aorta. For each aortic arch, the lesser curvature was cut open as well as the greater curvature where the branches (innominate artery, left common carotid and left subclavian) are. The aorta was then opened up and pinned down into a tray of wax. Figure 4.4 shows an aortic arch that has been opened and pinned into wax. Digital photographs were taken of every pinned aorta and the atherosclerotic lesions quantified as a percentage area of the aortic arch down until 3 mm from the base of the left subclavian artery. Lesions were defined as ivory-coloured fatty deposits within the arterial wall that had a raised profile, protruding into the lumen of the aorta. An atherosclerotic lesion is indicated by the blue arrow in figure 4.4. Figure 4.5 shows the mean atherosclerotic areas of the aortic arch in each *P. gingivalis*-inoculated group compared with their control littermates. Two-way ANOVA demonstrated no significant differences. It should be noted that few or no lesions were seen in the aortic arch in the majority of mice in all groups.

4.3.2 Aortic root atherosclerosis analysis

In this method of atherosclerosis analysis, nine cross sections of the aortic root 10μm thick were collected and stained with SUDAN IV and haematoxyllin. The section where the cusps disappeared (level 0) as well as the three sections of levels 100 μm, 200 μm, and 300 μm following were also examined for and the area of atherosclerotic lesions were

quantified. As an example, the sections labeled with Roman numerals i) through iv) in figure 3.2 highlight these four sections amongst the nine that were analyzed. As seen in figure 4.6, no differences between the groups of male mice were seen as confirmed by pairwise comparisons in a 3-way ANOVA. Figure 4.7A shows us that there appears to be no effect of *P. gingivalis* on IL-1β +/+ mice. There also appears to be no effect of IL-1β deficiency in non-inoculated control mice. It does appear as though there is a very strong trend towards more atherosclerotic lesions with inoculation of *P. gingivalis* in IL-1β -/- mice (*p=0.0065, where p<0.00625 to reach significance, analyzed by a pairwise comparison in three-way ANOVA). There also appears to be a strong trend towards an effect of IL-1β deficiency when mice are inoculated with *P. gingivalis* (†p=0.0067, where p<0.00625 to reach significance, analyzed by a pairwise comparison three-way ANOVA). In figure 4.7 B) Mean lesion areas at four different levels (Level 0, 100 μm, 200 μm, & 300 μm) within the aortic root of female mice showed that IL-1β-/- mice inoculated with *P. gingivalis* produced significantly increased lesion area compared to non-inoculated IL-1β-/- mice at level 0 (‡p=0.046, by one-way ANOVA).

Figure 4.4: En face analysis of atherosclerotic lesions in the aortic arch.
An atherosclerotic lesion is visible on the posterior side of this aortic arch, as indicated by the blue arrow. This aorta was taken from a male IL-1β -/- that had been inoculated with *P. gingivalis* and was the mouse that showed the greatest number of lesions and greatest lesion area. The scale is 1mm/unit.

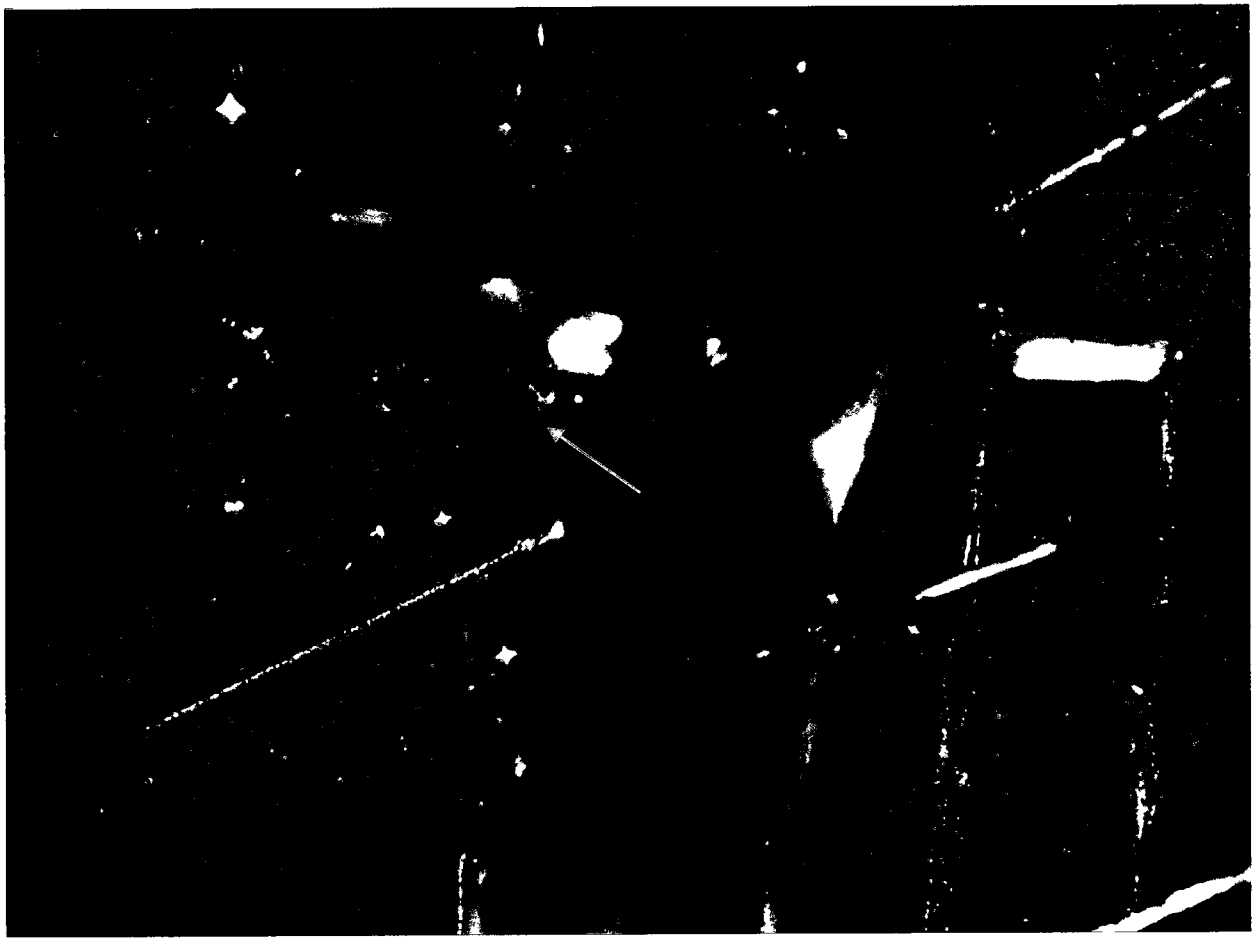

Figure 4.5: *En face* aortic lesion analysis of *P. gingivalis*-inoculated and control IL-1β+/+ and IL-1β-/- mice.

En face aortic arch lesion analysis demonstrating that the mean percent lesion area of aorta in each group in **A)** males and **B)** females, showed no significant difference in comparison of various groups.

A)

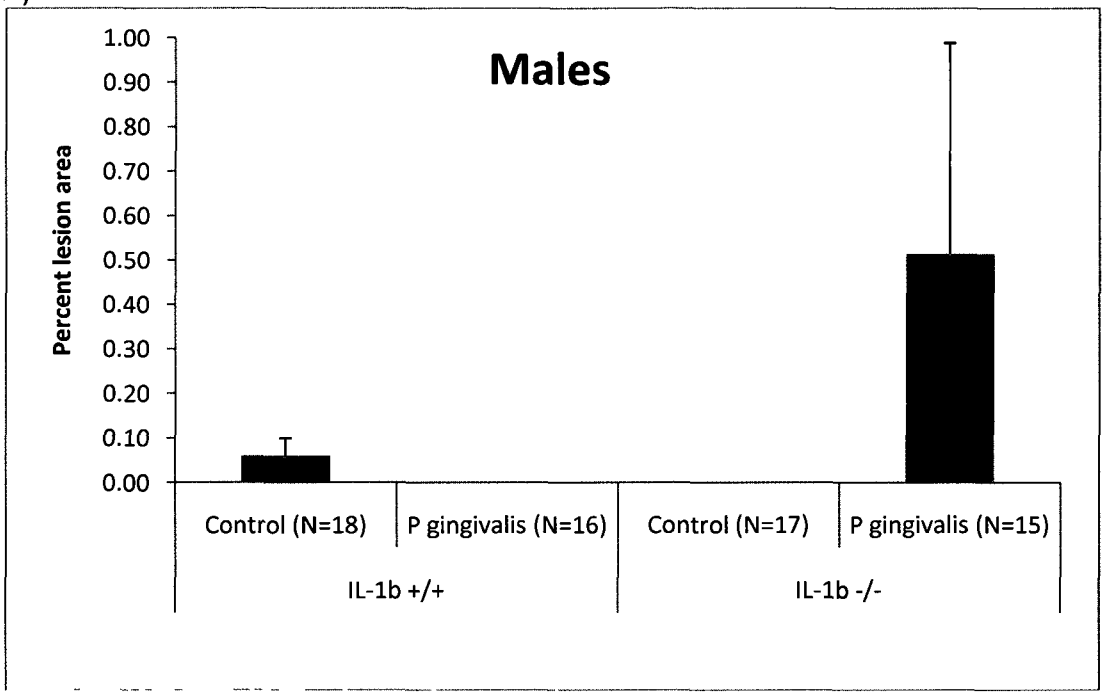
Males
Percent lesion area
1.00
0.90
0.80
0.70
0.60
0.50
0.40
0.30
0.20
0.10
0.00
Control (N=18)
P gingivalis (N=16)
Control (N=17)
P gingivalis (N=15)
IL-1b +/+
IL-1b -/-

B)

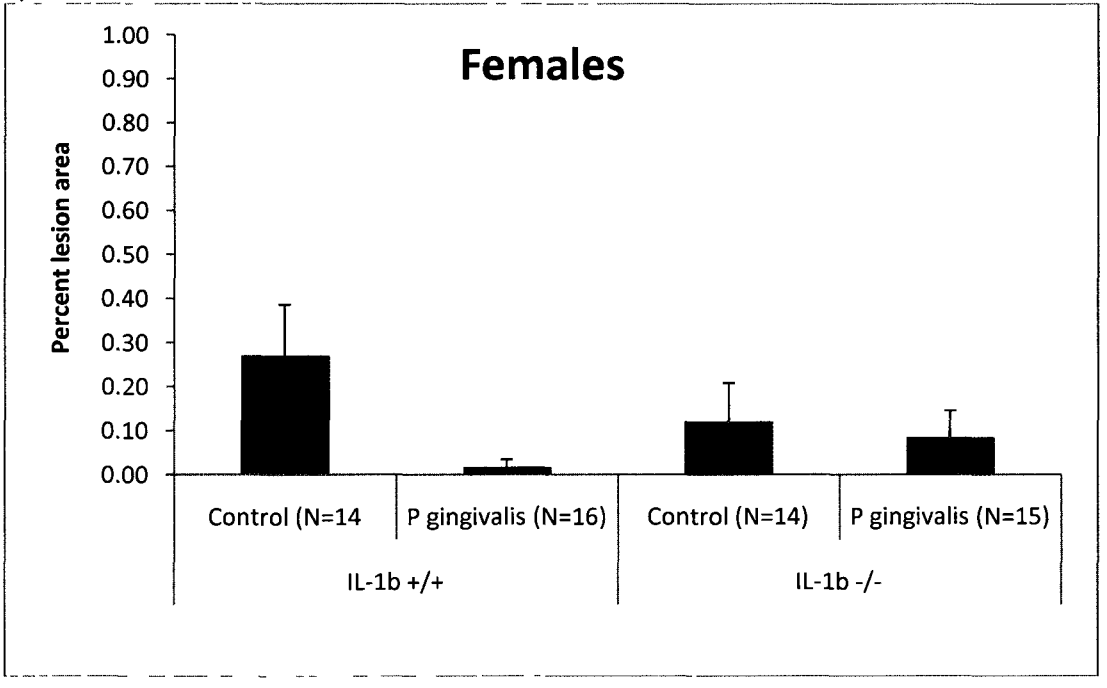
Females
Percent lesion area
1.00
0.90
0.80
0.70
0.60
0.50
0.40
0.30
0.20
0.10
0.00
Control (N=14
P gingivalis (N=16)
Control (N=14)
P gingivalis (N=15)
IL-1b +/+
IL-1b -/-

Figure 4.6: Quantification of atherosclerotic lesions in the aortic root of *P. gingivalis*-inoculated and control IL-1β+/+ and IL-1β-/- male mice.

A) Lesion area was calculated for each mouse as (lesion area at level 0 + lesion area at 100 μm + lesion area at 200 μm + lesion area at 300 μm) / 4. Error bars represent standard error. Pairwise comparisons in a 3-way ANOVA demonstrated no differences between the groups.

B) Mean lesion areas at four different levels (Level 0, 100 μm, 200 μm, & 300 μm) within the aortic root. Error bars represent standard error. No significant differences between groups were observed.

A)

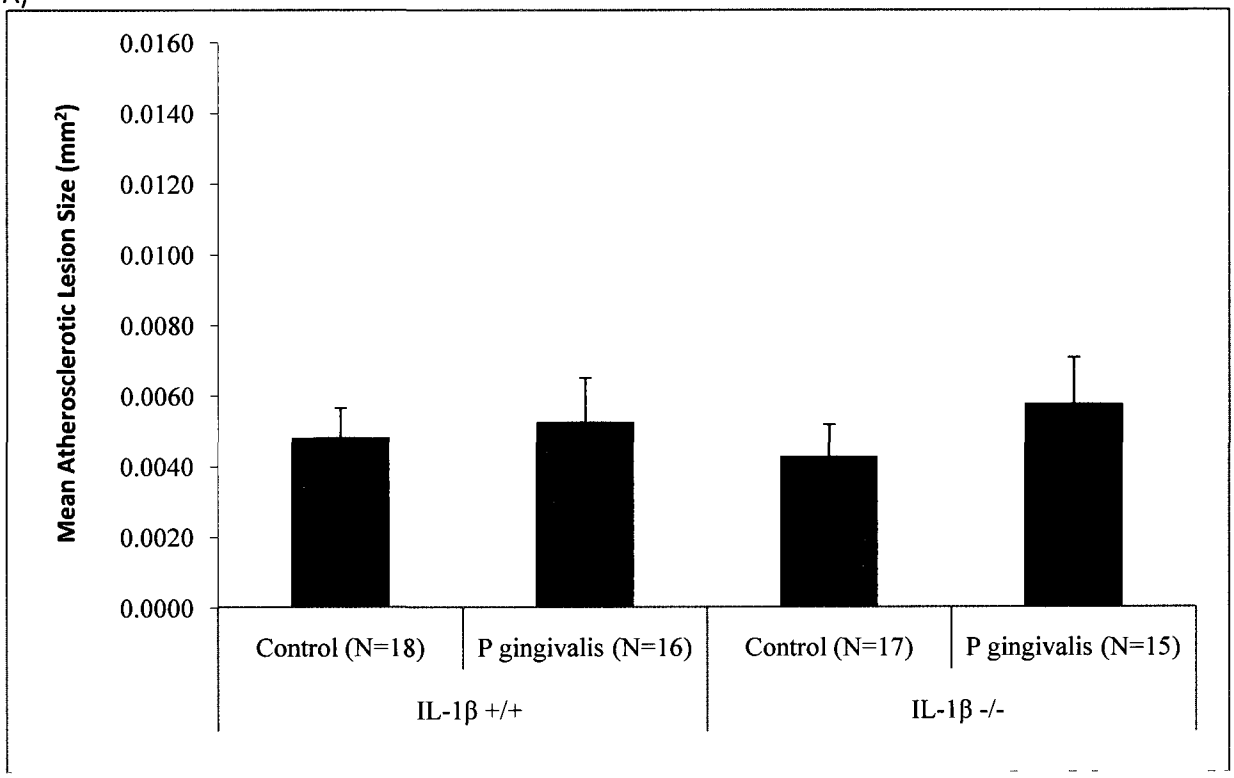
Mean Atherosclerotic Lesion Size (mm²)
0.0160
0.0140
0.0120
0.0100
0.0080
0.0060
0.0040
0.0020
0.0000
Control (N=18)
P gingivalis (N=16)
Control (N=17)
P gingivalis (N=15)
IL-1β +/+
IL-1β -/-

B)

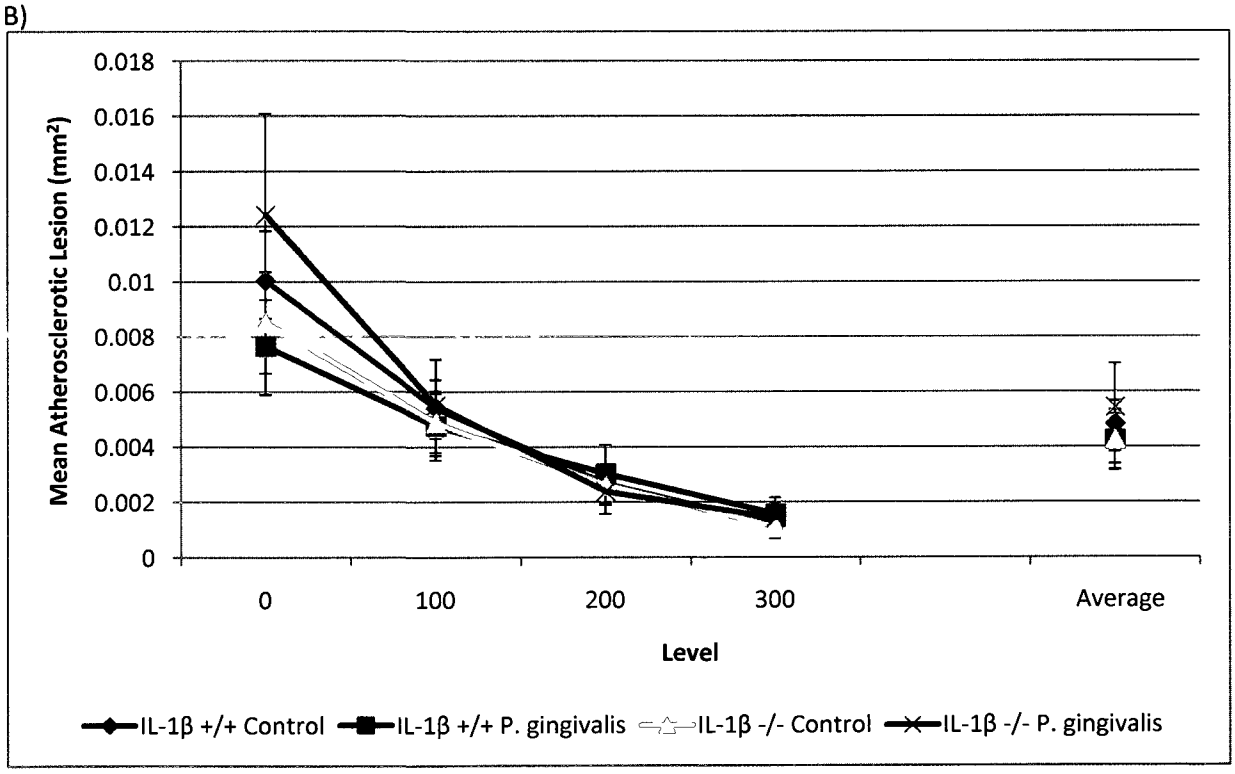
Mean Atherosclerotic Lesion (mm²)
0.018
0.016
0.014
0.012
0.01
0.008
0.006
0.004
0.002
0
0
100
200
300
Average
Level
IL-1β +/+ Control
IL-1β +/+ P. gingivalis
IL-1β -/- Control
IL-1β -/- P. gingivalis

Figure 4.7: Quantification of atherosclerotic lesions in the aortic root of *P. gingivalis*-inoculated and control IL-1β+/+ and IL-1β-/- female mice.

A) Lesion area was calculated for each mouse as (lesion area at level0 + lesion area at 100 μm + lesion area at 200 μm + lesion area at 300 μm) / 4. Error bars represent standard error. There appears to be no effect of *P. gingivalis* on IL-β +/+ mice. There also appears to be no effect of IL-1β deficiency in non-inoculated control mice. Error bars represent standard error. It does appear as though there is a very strong trend towards more atherosclerotic lesions upon inoculation of *P. gingivalis* in IL-β -/- mice (*p=0.0065, where p<0.00625 to reach significance, analyzed by a pairwise comparison in three-way ANOVA). There also appears to be a strong trend towards an effect of IL-β deficiency when mice are inoculated with *P. gingivalis* (†p=0.0067, where p<0.00625 to reach significance, analyzed by a pairwise comparison three-way ANOVA).

B) Mean lesion areas at four different levels (Level 0, 100 μm, 200 μm, & 300 μm) within the aortic root of female mice. Error bars represent standard error. IL-1β-/- mice inoculated with *P. gingivalis* show significantly increased lesion area compared to non-inoculated IL-1β-/- mice at level 0. (‡p=0.046, by one-way ANOVA)

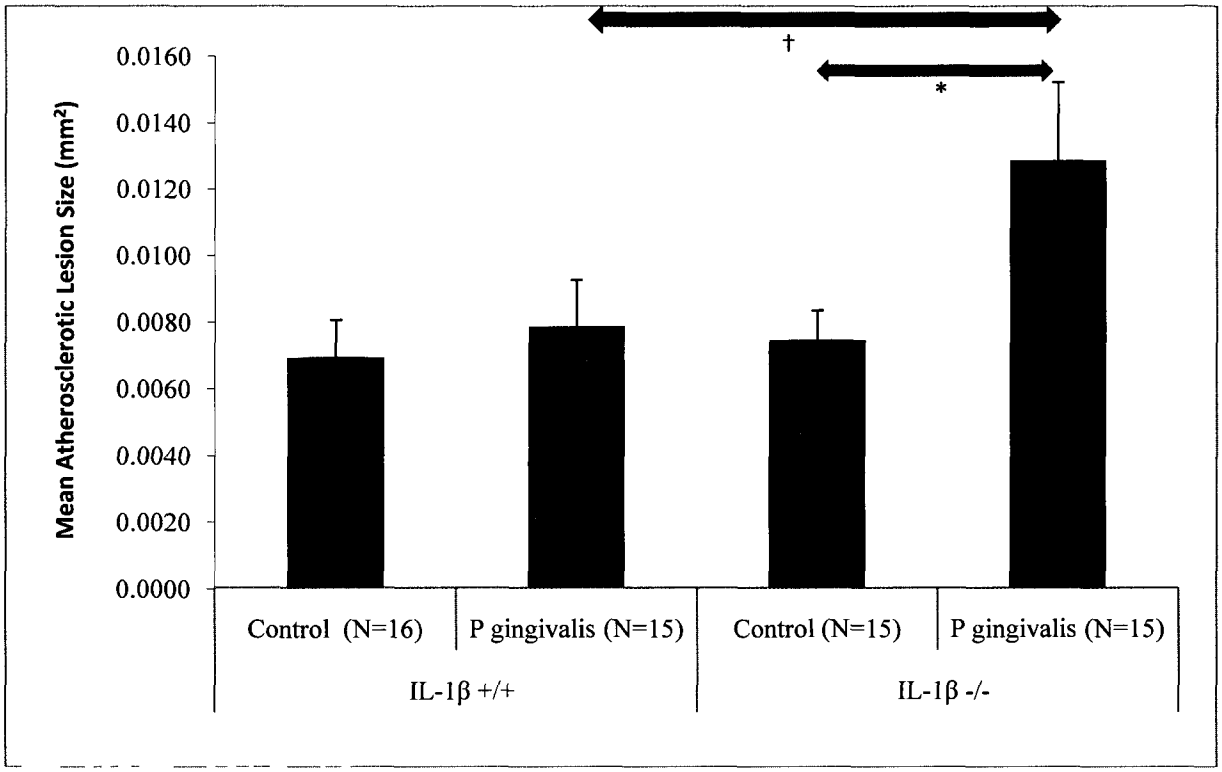
Mean Atherosclerotic Lesion Size (mm²)
0.0160
0.0140
0.0120
0.0100
0.0080
0.0060
0.0040
0.0020
0.0000
†
*
Control (N=16)
P gingivalis (N=15)
Control (N=15)
P gingivalis (N=15)
IL-1β +/+
IL-1β -/-

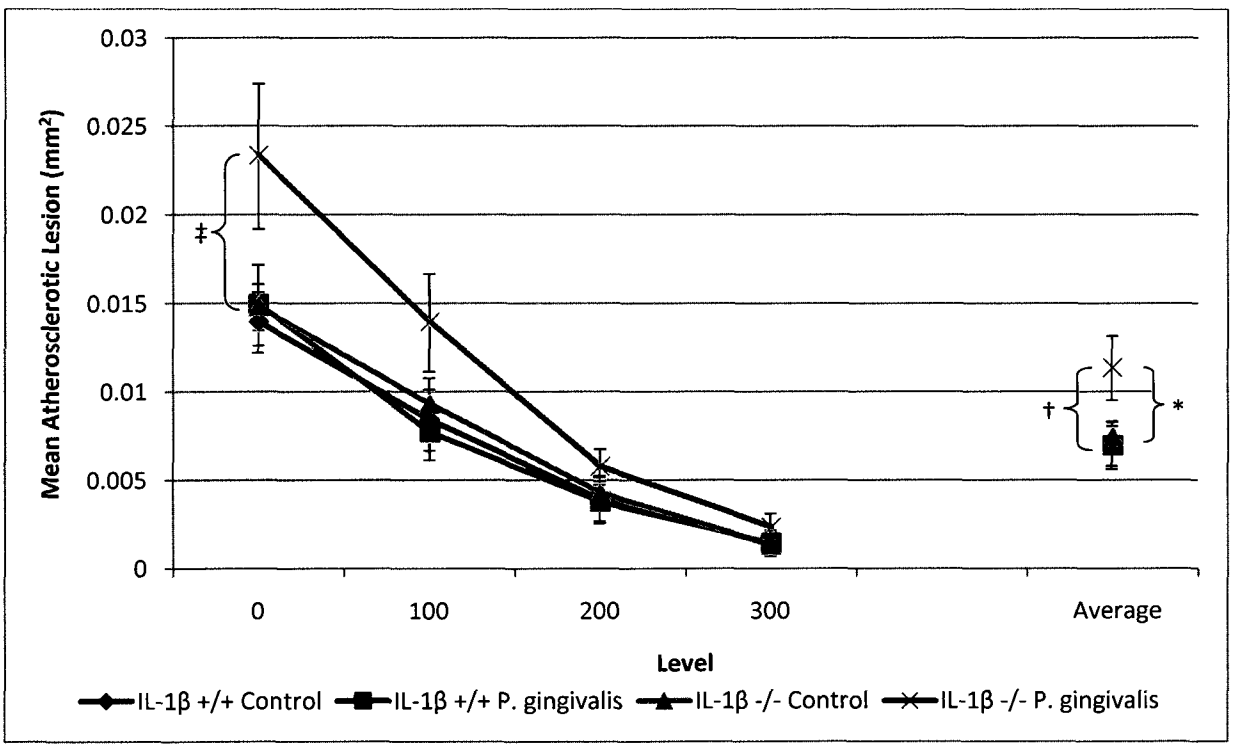
Mean Atherosclerotic Lesion (mm²)
0.03
0.025
0.02
0.015
0.01
0.005
0
‡
†
*
0
100
200
300
Average
Level
IL-1β +/+ Control
IL-1β +/+ P. gingivalis
IL-1β -/- Control
IL-1β -/- P. gingivalis

4.4 Systemic Host Response

The lack of an effect of *P. gingivalis* inoculation on alveolar bone loss and atherosclerosis, in the IL-1β+/+ apoE-/- mice was unanticipated in light of the previous work from the laboratory where increased alveolar bone loss and accelerated atherosclerosis was observed in *P. gingivalis*-inoculated apoE-/- mice when compared to non-inoculated littermates. One possibility was that the *P. gingivalis* inoculation in my study failed to establish an infection. To determine if a systemic infection had in fact occurred with *P. gingivalis* inoculations, we sought to demonstrate that sera from these mice had antibodies against *P. gingivalis*. To this end, an enzyme-linked immunosorbent assay (ELISA) was performed on four randomly chosen mouse sera per group to compare the *P. gingivalis* serum antibody titres of *P. gingivalis*-inoculated and control IL-1β+/+apoE-/- and IL-1 β-/-apoE-/- mice (figure 4.8).

Since, in the earlier caspase-1 study, it was observed that caspase-1+/+ apoE-/- mice (i.e. the same genotype as our IL-1β+/+ apoE-/- mice) had increased bone loss and increased atherosclerosis compared to non-inoculated littermates, we also measured anti-*P. gingivalis* titres in sera from *P. gingivalis*-inoculated and control caspase-1+/+ apoE-/- (4 sera samples / group) from this earlier study to serve as a control for our present study (figure 4.9). It is evident from the results shown in figure 4.8 that IL-1β+/+ and IL-1β-/- mice which had been inoculated with *P. gingivalis* mounted a strong humoral anti-*P. gingivalis* immune response. Moreover, the anti-*P. gingivalis* titres observed in the present study (figure 4.8) were similar to those which we detected in sera from *P. gingivalis*-inoculated mice from the earlier caspase 1 study (figure 4.9). Therefore, our inability to

show increased bone loss and accelerated atherosclerosis in the *P. gingivalis*-inoculated mice cannot be attributed to a failure to establish an infection in the inoculated mice.

Figure 4.8: Antibody titres in *P. gingivalis*-inoculated mice compared to the non-inoculated mice of both IL-1β +/+ and IL-1β -/- genotypes.

An ELISA was performed on **A)** male & **B)** female *P. gingivalis*-inoculated and non-inoculated IL-1β +/+ and -/- mice sera, demonstrating the higher antibody titres in the *P. gingivalis*-inoculated mice compared to the non-inoculated mice.

Repeated measures analysis comparing the two slopes of the infected mice showed no statistically significant differences in the males but do in the females (*$p<0.001$).

A)

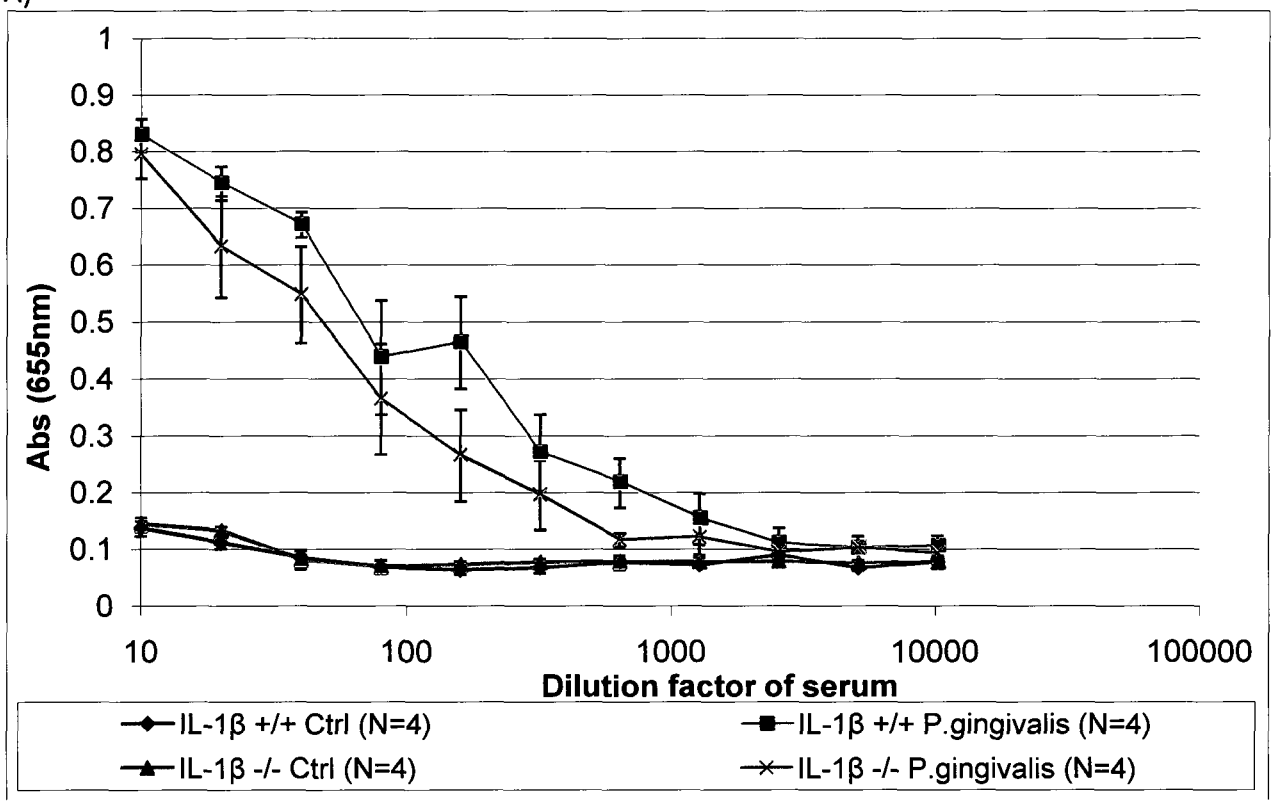
1
0.9
0.8
0.7
0.6
0.5
0.4
0.3
0.2
0.1
0
Abs (655nm)
10
100
1000
10000
100000
Dilution factor of serum
IL-1β +/+ Ctrl (N=4)
IL-1β +/+ P.gingivalis (N=4)
IL-1β -/- Ctrl (N=4)
IL-1β -/- P.gingivalis (N=4)

B)

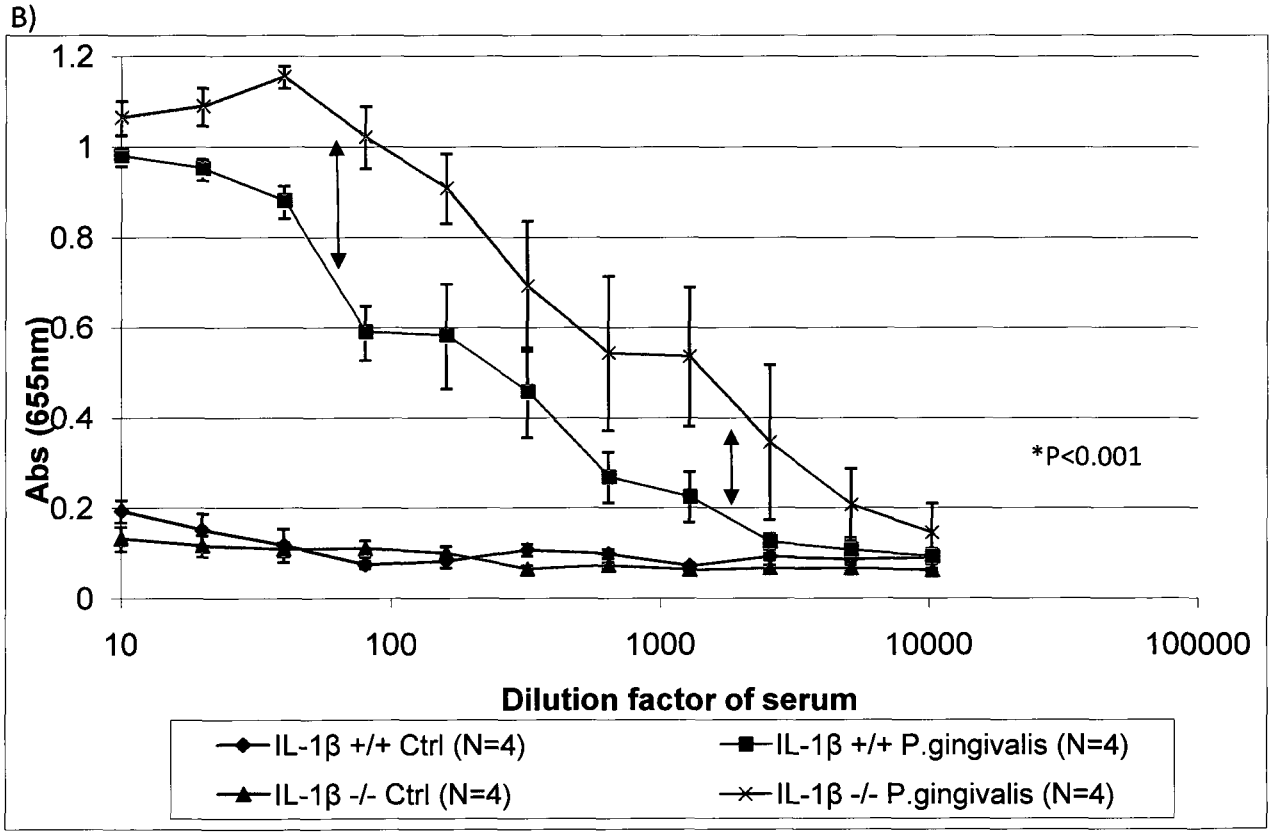
1.2
1
0.8
0.6
0.4
0.2
0
Abs (655nm)
*P<0.001
10
100
1000
10000
100000
Dilution factor of serum
IL-1β +/+ Ctrl (N=4)
IL-1β +/+ P.gingivalis (N=4)
IL-1β -/- Ctrl (N=4)
IL-1β -/- P.gingivalis (N=4)

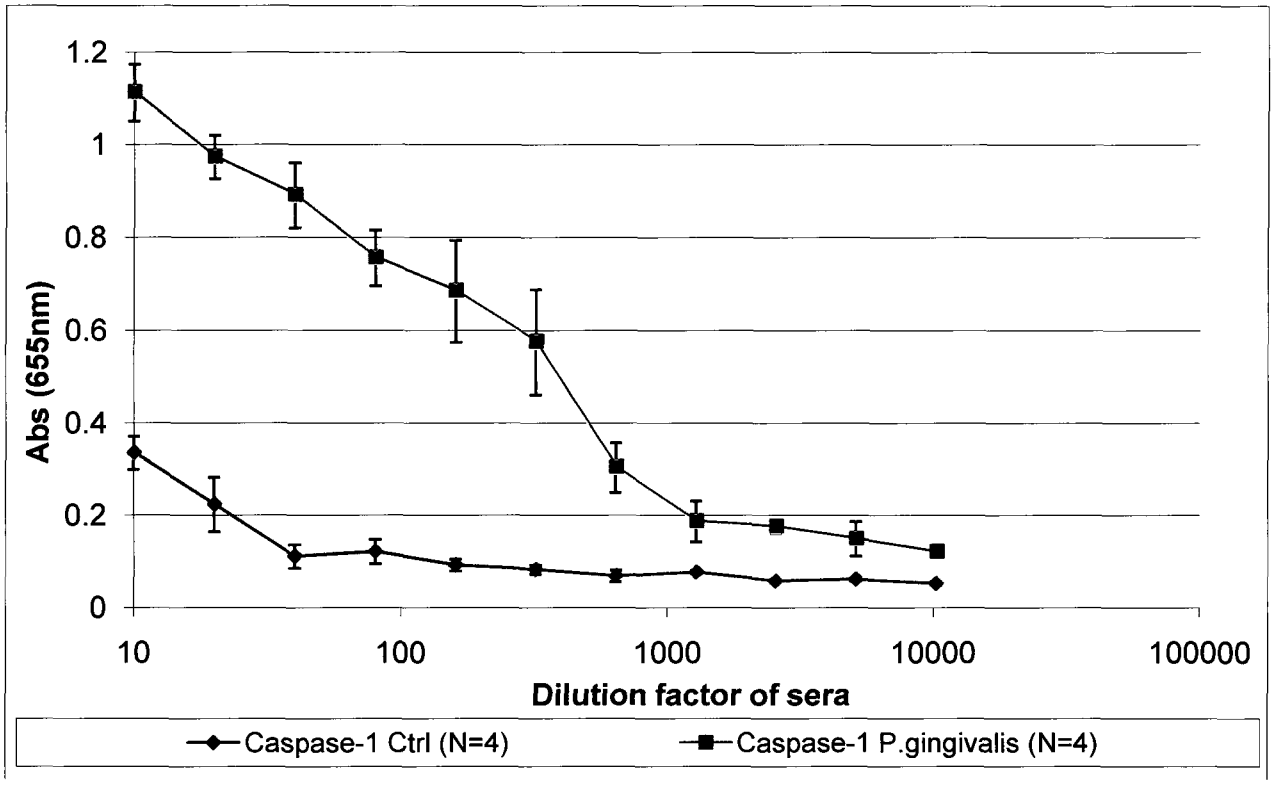
1.2
1
0.8
0.6
0.4
0.2
0
Abs (655nm)
10
100
1000
10000
100000
Dilution factor of sera
Caspase-1 Ctrl (N=4)
Caspase-1 P.gingivalis (N=4)

Figure 4.9: Antibody titres in caspase-1 +/+ male mice,
P. gingivalis-inoculated compared to non-inoculated littermates. An ELISA was performed on male *P. gingivalis*-inoculated and non-inoculated caspase-1 +/+ apoE -/- mice sera, demonstrating the higher antibody titres in the *P. gingivalis*-inoculated mice compared to the non-inoculated mice.

5. Discussion

Ever increasing evidence is pointing towards periodontal disease as being a contributor to various systemic diseases such as atherosclerosis and diabetes (Gibson et al., 2006). Amongst the more than 500 different bacterial species identified in the oral cavity, *P. gingivalis* is the species most commonly associated with periodontal disease in adults. The Genco group has shown that for periodontal disease to accelerate atherosclerosis, invasive bacterial species are needed. Bacterial species associated with periodontal disease, including *P. gingivalis,* have been found to exist in the walls of atherosclerotic vessels (Gibson et al., 2006). The presence of bacteria in the artery wall can potentially stimulate a local inflammatory response with the production of cytokines such as IL-1β. Invasive *P. gingivalis* has been shown to up-regulate chemokine expression as well as cell adhesion molecules, in both endothelial cells and macrophages (Gibson et al., 2006). In macrophages, IL-1β expression is upregulated upon exposure to live *P. gingivalis* (Zhou and Amar, 2007; Bodet et al., 2006). Thus, in addition to modified lipoproteins, local and or distant infections with bacteria such as *P. gingivalis* are thought to contribute to the inflammatory process that occurs during atherosclerosis development.

The goal of my project was to gain insight into the mechanistic relationship between periodontal disease and atherosclerosis using a mouse model. Previously obtained data from the Whitman laboratory demonstrated that, in apoE-/- mice, caspase-1 is required for *P. gingivalis*-accelerated atherosclerosis (Gage et al., unpublished results). Caspase-1 is responsible for activating IL-1β as well as IL-18. IL-1β deficiency *in vivo* has been shown to

significantly reduce atherosclerosis in atherosclerosis-susceptible mouse models (Kirii et al., 2003). Based on these premises, I set out to test the hypothesis that caspase-1 activation of IL-1β was responsible for the accelerated atherosclerosis seen in *P. gingivalis*-inoculated apoE-/- mice. To this end, I have quantified atherosclerotic lesions in the aortic root and aortic arch of control IL-1β+/+apoE-/- and IL-1β-/-apoE-/- mice and in IL-1β+/+apoE-/- and IL-1β-/-apoE-/-that had been orally inoculated with *P. gingivalis*. To monitor periodontal disease in the mice, I have measured mandibular bone loss. Since caspase-1 also activates IL-18, a parallel study was conducted in the Whitman laboratory to examine the role of IL-18 in *P. gingivalis*-accelerated atherosclerosis in apoE -/- mice.

There are several established risk factors which potentially contribute to the development of atherosclerosis and could be altered by either IL-1β genotype or by *P. gingivalis* infection. It has been previously shown that glucose, insulin and creatinine levels were not altered in mice following *P. gingivalis* treatment (Lalla et al., 2003). As can be seen in figures 4.1 and 4.2, we found that serum cholesterol levels and the distribution of cholesterol within the lipoprotein fractions were similar in IL-1β+/+apoE-/- and IL-1β-/-apoE-/- mice and were not changed by *P. gingivalis* inoculation. As would be anticipated with apoE-/- mice the cholesterol was predominantly in the VLDL fraction. While there was a difference in the VLDL peak between inoculated and non-inoculated IL-1β +/+ mice of both genders ($p=0.04$), the biological significance of this difference may be questioned as sera from only 5-7 mice / group were subjected to FPLC separation. The sera that were analyzed for each group were chosen at random and may not be representative the entire

group in terms of total serum cholesterol levels. The lack of difference between groups in terms of plasma cholesterol levels and the similarity in lipoprotein profiles would suggest that any differences that are observed in terms of atherosclerosis are not due to changes in serum lipids or lipoproteins caused by IL-1β genotype or inoculation with *P. gingivalis.*

This research project was carried out to gain further insight into the mechanisms underneath the relationship between periodontal disease and atherosclerosis. To this end we attempted to establish that there was indeed a chronic oral infection. Since alveolar bone loss has already been established as a hallmark for periodontal disease, we sought to quantify the amount of bone regression in the mandibles of the study mice. Non-infected IL-1β deficient mice compared to non-infected IL-1β competent mice demonstrated that IL-1β was involved in promoting periodontal disease. Performing two-way ANOVA demonstrated significantly less bone loss in male mice ($p=0.024$) and a trend in the female mice ($p=0.0266$). To further support this, a three-way ANOVA showed that the alveolar bone loss observed was significantly attenuated due to IL-1β deficiency irrespective of gender ($p=0.0014$). The data collected supports the notion that IL-1β deficiency would reduce the amount of alveolar bone loss due to an attenuated inflammatory response in the gingival tissue regardless of whether the mice were infected with *P. gingivalis* or not.

It was also expected that the administration of *P. gingivalis* would significantly increase alveolar bone loss in IL-1β competent apoE-/- mice. However, neither the males nor the females showed any difference in alveolar bone loss with *P. gingivalis* inoculation compared to their non-infected control littermates of the same genotype. This was contrary to what was previously shown in our laboratory. In this study apoE-/- mice

inoculated with *P. gingivalis* were shown to have an increase in bone loss compared to non-inoculated controls (Gage et al. unpublished results). A simple explanation for our inability to demonstrate increased bone loss in the *P. gingivalis*-inoculated mice would be that we failed to establish either a local or a systemic infection with our inoculation procedure. To determine if infection did occur in the inoculated mice, anti-*P. gingivalis* antibodies in the sera of inoculated and control mice were measured using an ELISA. *P. gingivalis*-inoculated mice showed significantly increased titres of antibodies compared to their non-inoculated littermates and this was the case for both IL-1β+/+ apoE-/- and IL-1β-/- apoE-/- mice (Figure 4.8). Curiously, inoculated female IL-1β-/- apoE-/- mice appeared to mount a stronger anti-*P. gingivalis* humoral immune response than did inoculated IL-1b+/+ apoE-/- females. This difference was not seen in males. It should be underlined that the sera of only four mice per group were assayed for anti-*P. gingivalis* antibodies. Although the method of inoculation differed from that which we used (see below), Lalla et al. also detected anti-*P. gingivalis* antibody in the sera of inoculated mice (Lalla et al., 2003). Given the apparent discrepancy between my results and the earlier study from the laboratory (Gage et al., unpublished results), I also used the ELISA to quantify anti-*P. gingivalis* antibodies in sera from this earlier study (Figure 4.9). Inoculation of Caspase-1+/+ apoE-/- (the same genotype as the IL-1β+/+ apoE-/- mice) with *P. gingivalis* elicited a humoral immune response similar to which we observed in my study. Therefore, the inability to demonstrate increased alveolar bone loss in the inoculated mice cannot be attributed to a failure to establish an infection with the *P. gingivalis*.

Similar to the earlier results from the Whitman lab (Gage et al., unpublished results), Lalla et al. (2003) also showed increased alveolar bone loss in *P. gingivalis*-inoculated mice compared to non-inoculated controls. In this case, the discrepancy likely results from differences in the inoculation technique. Lalla *et al.* (2003) used carboxymethylcellulose as a base to suspend the *P. gingivalis* to infect their mice both an oral and an anal route. The use of carboxymethylcellulose likely increased bacterial adherence and the combined inoculation routes may have increased effective bacterial infection dose. In addition, Lalla et al. (2003) compared 21 mice per group. The contradictions between my results and those of Gage et al. (unpublished results) are more difficult to explain as identical inoculation protocols were used in the two studies. One possibility is that functional mutations in the *P. gingivalis* genome arose with time or that there was contamination of the *P. gingivalis* that was used for inoculation. It is notable that in the earlier study, the *P. gingivalis* cultures were analyzed weekly by PCR to confirm the presence of *P. gingivalis* but purity of the cultures was not regularly confirmed. During the course of my study, samples of the *P. gingivalis* cultures were sent weekly to the clinical microbiology diagnostic lab of the Ottawa Hospital, General Campus to test for purity. When contaminants were detected, affected bacterial cultures were immediately bleached and any mice inoculated with contaminated cultures were excluded from the study. Had there been contamination with at least another strain of bacteria, the results would support the idea that a multiple pathogen infection is more effective in creating periodontal disease. Findings by Kuramitsu et al show that *P. gingivalis* strain 381 can form a cooperative relationship with *Treponema denticola* strain 35405 (Kuramitsu et al., 2005). This synergistic relationship relied on gene

expression by the other bacterium to successfully produce a biofilm (Kuramitsu et al., 2005).

The lack of increased bone loss in the IL-1β competent mice perhaps may be due to the fact that extracellular bacterial antigens generally favour a Th2 response. A Th2 response does not promote bone resorption, in contrast to a Th1 response (Stashenko et al., 2007). Th2 cytokines are known to inhibit macrophage activation and as such would prevent foam cell formation and atherosclerosis development. This possibility could be explored in future studies. Findings by Berker et al support this notion, as they were able to show that monocytes increased IL-10 production in the presence of apoptotic neutrophils (Berker et al., 2005). They also were able to show that IL-1β was significantly repressed in monocytes cultured with either fresh or apoptotic neutrophils. Additional experiments demonstrated that monocytes, co-cultured with apoptotic neutrophils, stimulated with *P. gingivalis* LPS produced significantly less IL-1β than without any neutrophils (Berker et al., 2005).

En face analysis of the mice at 17 weeks of age showed no difference in the amount of atherosclerosis within the aortic arch between any of the treatment groups. Referring to figure 4.5, neither *P. gingivalis* inoculation nor IL-1β deficiency had any effect on lesion size. Consistent in both genders, these results are also consistent with previous results obtained by Gage, in the caspase-1 study. These aortas had very little to no lesions with the majority of them showing no lesions at all. This is a direct result of not putting the mice

on a high fat/high cholesterol diet. Alternatively, increasing the age of the mice at the time of sacrifice would also increase the amount of atherosclerosis seen in the aortic arch.

We also quantified atherosclerosis in the aortic root. As seen in figures 4.6 and 4.7, results indicated that there was no significant difference between IL-1β +/+ apoE -/- control mice and their *P. gingivalis*-inoculated littermates in both male and females. This may not be surprising as we did not see a difference in mandibular bone loss between inoculated and control mice. Other factors may also, in part, account for our failure to observe increased atherosclerosis in the inoculated mice. Lalla et al employed an n value of 25 apoE deficient mice per group (Lalla et al., 2003) and perhaps if our n values were increased, there may be significant differences. In the event that the bacterial cultures used in the earlier study by Gage et al. (unpublished) were indeed contaminated, that would support the notion that increased pathogen burden increases the inflammatory response and in due course, increased atherosclerosis. It is notable that, in a study carried out in parallel with mine in the Whitman laboratory to examine the role of IL-18 in *P. gingivalis* accelerated atherosclerosis, no increase in atherosclerotic lesions in the *P. gingivalis*-inoculated mice compared to non-inoculated mice (unpublished results) was observed, thus confirming my results.

As we failed to see increased bone loss or increased atherosclerosis in the *P. gingivalis*-inoculated mice, we considered the possibility that the mice had suffered from periodontal disease even in the absence of *P. gingivalis* inoculation. We, therefore, pooled the alveolar bone loss data and aortic root lesion area for a given genotype and sex

regardless of *P. gingivalis* infection and plotted lesion area as function of bone loss. As shown in figure 5.1, no correlation was seen.

In the male IL-1β -/- mice showed no reduction in aortic root atherosclerotic lesion sizes compared to their IL-1β +/+ littermates with N values of 17 and 18 respectively. While this appears to contradict what Kirii et al was able to demonstrate with just N values of 9 that IL-1β deficiency reduces aortic root atherosclerotic lesion sizes by approximately 32% in both 12 week model as well as the 24 week model. We must keep in mind however that Kirii et al used a different method of measurement to quantify aortic root lesions. They selected a mid-cusp section, and then acquired its image along with the image of 100μm before and 100μm after. The lesion size measured per mouse is the sum of all three selected sections. The area of the aortic sinus spanning 400μm following the disappearance of the cusps was found by Paigen et al to be the most reliable area to measure atherosclerotic lesions in the aortic root (Paigen et al., 1987).

Much to our surprise however, figure 4.7 shows us that the mean atherosclerotic lesion size of the *P. gingivalis*-inoculated female IL-1β deficient mice was borderline to being significantly higher than that of their IL-1β deficient control sisters (*$p=0.0065$, where $p<0.00625$ to reach significance, analyzed by a pairwise comparison in three-way ANOVA) as well as their inoculated IL-1β +/+ littermates (†$p=0.0067$, where $p<0.00625$ to reach significance, analyzed by a pairwise comparison three-way ANOVA). In figure 4.7B, IL-1β-/- mice inoculated with *P. gingivalis* show significantly increased lesion area

compared to non-inoculated IL-1β-/- mice at level 0. (‡p=0.046, by one-way ANOVA). This was in contrast to our hypothesis that inoculating IL-1β deficient mice would not increase atherosclerosis. These results indicate to us that in the absence of IL-1β, there appears to be a compensatory mechanism that is engaged following *P. gingivalis* inoculations. There appears to be no significant difference in mean atherosclerotic lesion sizes between IL-1β deficient males that were inoculated and those that were not. Given the trends seen, we will not exclude the possibility that significance may be reached with increased N values to increase the power.

Perhaps an alternative pathway is activated in the absence of IL-1β. Kanneganti and her research team recently found that caspase-1 deficiency protected mouse bone marrow derived macrophages (BMDM) from developing sepsis (Kanneganti, 2010). However when the same experiment was carried over into IL-18 or IL-1β deficient BMDMs, they were no longer protected. Suggesting that there must be other substrates for caspase-1, the Kanneganti group found that activation of caspase-7 and the high mobility group protein B1 (HMGB1) were both downstream of caspase-1 and absolutely necessary for sepsis to manifest itself (Kanneganti, 2010). While this does not explain why there is a significant increase in atherosclerosis in the inoculated mice, it gives us insight into the idea that there may be a compensatory mechanism that is activated we do not yet know about. This is definitely an area that warrants further study. Other recent findings by Mayer-Barber et al have shown that mice did not require TLR or caspase-1 in their production of IL-1β following infection with *Mycobacterium tuberculosis* (Mayer-Barber et al., 2010). Contrary

to what one would expect, IL-1β-deficient mice showed significant infection susceptibility compared to mice deficient in caspase-1 or MyD88. This demonstrates that a caspase-1 deficient study may not produce the same results as an identical IL-1β deficient study and that much of the proinflammatory pathways are not well understood.

Figure 5.1: Correlation plot of atherosclerotic lesion sizes against alveolar bone loss in males.

In attempts to demonstrate a correlation between alveolar bone loss and atherosclerosis, values of aortic root atherosclerotic lesion sizes were plotted against the alveolar bone loss value of the respective mouse. No correlation was observed.

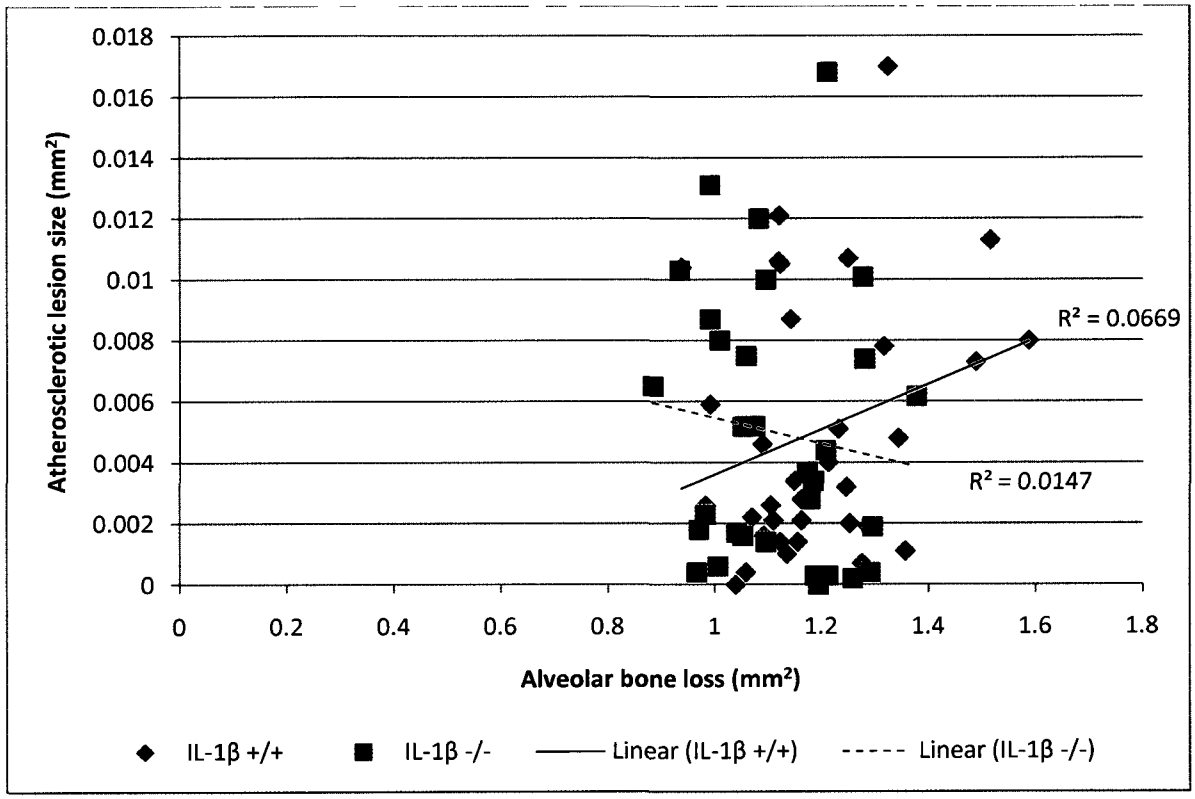
0.018
0.016
0.014
0.012
0.01
0.008
0.006
0.004
0.002
0
Atherosclerotic lesion size (mm²)
0
0.2
0.4
0.6
0.8
1
1.2
1.4
1.6
1.8
Alveolar bone loss (mm²)
R² = 0.0669
R² = 0.0147
IL-1β +/+
IL-1β -/-
Linear (IL-1β +/+)
Linear (IL-1β -/-)

5.1 Conclusion

Working towards uncovering the biochemical pathways for *P. gingivalis*-promoted atherosclerosis is important in understanding how an oral infection can contribute to cardiovascular disease. In this study, we used IL-1β+/+ apoE-/- and IL-1β-/- apoE-/- mice to determine whether or not IL-1β is required for alveolar bone loss and atherosclerosis development that is accelerated by a chronic oral infection of with *P. gingivalis*. We observed that alveolar bone loss was significantly reduced in the apoE-/-IL-1β mice. This supports our hypothesis that IL-1β plays an important role in the pathogenesis of periodontal disease. However, in contrast to earlier observations from the laboratory, *P. gingivalis* inoculation did not increase alveolar bone loss in the mice. Successful infection was confirmed in the *P. gingivalis*-inoculated mice and we propose that the discrepancies with the earlier study may result from introduction of mutations into the *P. gingivalis* stock that may alter its invasive properties or contamination of the *P. gingivalis* cultures used in the earlier experiments. Our second hypothesis, that apoE-/- mice deficient in IL-1β given oral inoculations of *P. gingivalis* will show less atherosclerotic lesions than their IL-1β competent littermates, was not supported by the data. As was the case for alveolar bone loss, *P. gingivalis* infection did not accelerate atherosclerosis. This was also in contrast to the earlier study and again may be the result of genetic changes in *P. gingivalis* that occurred over time or contamination of the *P. gingivalis* cultures used in the previous study. Atherosclerotic lesions did not differ between male IL-1β+/+ apoE-/- and male IL-1β-/- apoE-/- mice. Surprisingly, in females there was a very strong trend towards IL-1β deficiency actually promoting atherosclerosis following infection ($p=0.0067$, where

$p<0.00625$ to reach significance) in direct contrast to my starting hypothesis. Further experiments are required to determine if there is, in fact, a gender difference. I propose that an alternative pathway may be activated upon infection of *P. gingivalis* in the absence of IL-1β.

5.2 Future Directions

While this study was not able to reproduce all of the results that have been seen by others, it has given us insight into something new regarding the biochemistry behind the *P. gingivalis*-accelerated atherosclerosis model. To confirm the results of this study, we suggest increasing the N values. Working in an *in vivo* model such as the mouse, can be difficult at times and other unexpected factors may play a role in influencing the study. To this end, we believe that increasing the N values would increase the power of the study and provide us with more definitive results. Likewise, it will be important to identify the causes responsible for our inability to observe the increased alveolar bone loss and increased atherosclerosis in *P. gingivalis*-inoculated apoE-/- that had been seen in the previous study in the laboratory.

We also suggest exploring gender differences. *P. gingivalis*-inoculated apoE-/-IL-1β -/- female mice show such a strong trend towards accumulating more atherosclerotic lesions compared to their inoculated IL-β +/+ littermates. If these results are an indication of anything, it would be that there is an alternate mechanism that a systemic *P. gingivalis* infection can activate when the mice are unable to produce IL-1β. A recently discovered

cytokine, IL-33 is a Th2 promoting cytokine, that can attenuate foam cell formation and there is debate as to whether caspase-1 is responsible in activating it or not. If IL-33 is indeed processed by caspase-1, this could also explain why my results differed from the caspase-1 study. If it is not, it still may be worthwhile to further elucidate its role in *P. gingivalis*-associated atherosclerosis development.

Additionally, we propose looking at a broader perspective such as investigating the association of periodontal disease and cardiovascular disease and how diabetes can play a role in mediating between these two diseases. Studies over the past few years have shown that receptors for advanced glycation end products (RAGE) are involved in periodontitis-linked diabetes as well as cardiovascular disease. The mechanism of how this occurs is not completely understood, therefore warrants future attention.

6. References

Adiels, M., Olofsson, S., Taskinen, M., and Borén, J. (2008). Overproduction of very low-density lipoproteins is the hallmark of the dyslipidemia in the metabolic syndrome. Arterioscler. Thromb. Vasc. Biol *28*, 1225-1236.

Barksby, H. E., Lea, S. R., Preshaw, P. M., and Taylor, J. J. (2007). The expanding family of interleukin-1 cytokines and their role in destructive inflammatory disorders. Clin. Exp. Immunol *149*, 217-225.

Berker, E., Kantarci, A., Hasturk, H., and Van Dyke, T. E. (2005). Effect of neutrophil apoptosis on monocytic cytokine response to Porphyromonas gingivalis lipopolysaccharide. J. Periodontol *76*, 964-971.

Bodet, C., Chandad, F., and Grenier, D. (2006). Porphyromonas gingivalis-induced inflammatory mediator profile in an ex vivo human whole blood model. Clin. Exp. Immunol *143*, 50-57.

Breslow, J. (1995). Familial disorders of high-density lipoprotein metabolism. In The Metabolic and Molecular Bases of Inherited Disease (New York: Mcgraw-Hill), pp. 1015-1076.

Burns, E., Bachrach, G., Shapira, L., and Nussbaum, G. (2006). Cutting Edge: TLR2 is required for the innate response to Porphyromonas gingivalis: activation leads to bacterial persistence and TLR2 deficiency attenuates induced alveolar bone resorption. J. Immunol *177*, 8296-8300.

Case, C. L., Shin, S., and Roy, C. R. (2009). Asc and Ipaf Inflammasomes Direct Distinct Pathways for Caspase-1 Activation in Response to Legionella pneumophila. Infect. Immun. *77*, 1981-1991.

Daugherty, A., and Whitman, S. C. (2003). Quantification of atherosclerosis in mice. Methods Mol. Biol *209*, 293-309.

Desvarieux, M., Demmer, R. T., Rundek, T., Boden-Albala, B., Jacobs, D. R., Papapanou, P. N., and Sacco, R. L. (2003). Relationship between periodontal disease, tooth loss, and carotid artery plaque: the Oral Infections and Vascular Disease Epidemiology Study (INVEST). Stroke *34*, 2120-2125.

Desvarieux, M., Demmer, R. T., Rundek, T., Boden-Albala, B., Jacobs, D. R., Sacco, R. L., and Papapanou, P. N. (2005). Periodontal microbiota and carotid intima-media thickness: the Oral Infections and Vascular Disease Epidemiology Study (INVEST). Circulation *111*, 576-582.

Dinarello, C. A. (1996). Biologic basis for interleukin-1 in disease. Blood *87*, 2095-2147.

Dinarello, C. A. (1997). Interleukin-1. Cytokine Growth Factor Rev *8*, 253-265.

Dinarello, C. A. (2009). Immunological and inflammatory functions of the interleukin-1 family. Annu. Rev. Immunol *27*, 519-550.

Dorn, B. R., Burks, J. N., Seifert, K. N., and Progulske-Fox, A. (2000). Invasion of endothelial and epithelial cells by strains of Porphyromonas gingivalis. FEMS Microbiol. Lett *187*, 139-144.

Dorn, B. R., Dunn, W. A., and Progulske-Fox, A. (1999). Invasion of human coronary artery cells by periodontal pathogens. Infect. Immun *67*, 5792-5798.

Fabricant, C. G., Fabricant, J., Litrenta, M. M., and Minick, C. R. (1978). Virus-induced atherosclerosis. J. Exp. Med *148*, 335-340.

Floudas, C. (2007). Computational methods in protein structure prediction. Biotechnology and Bioengineering *97*, 207-213.

Franchi, L., Stoolman, J., Kanneganti, T., Verma, A., Ramphal, R., and Núñez, G. (2007). Critical role for Ipaf in Pseudomonas aeruginosa-induced caspase-1 activation. Eur. J. Immunol *37*, 3030-3039.

Friedewald, V. E., Kornman, K. S., Beck, J. D., Genco, R., Goldfine, A., Libby, P., Offenbacher, S., Ridker, P. M., Van Dyke, T. E., and Roberts, W. C. (2009). The American Journal of Cardiology and Journal of Periodontology Editors' Consensus: periodontitis and atherosclerotic cardiovascular disease. Am. J. Cardiol *104*, 59-68.

Gage, J., Hasu, M., Burchat, S., and Whitman, S. The Periodontal Pathogen, Porphyromonas gingivalis and the Participatory Role of Caspase-1 in the Progression of Atherosclerosis.

Gibson, F. C., Yumoto, H., Takahashi, Y., Chou, H., and Genco, C. A. (2006). Innate immune signaling and Porphyromonas gingivalis-accelerated atherosclerosis. J. Dent. Res *85*, 106-121.

Gibson, F. C., Hong, C., Chou, H., Yumoto, H., Chen, J., Lien, E., Wong, J., and Genco, C. A. (2004). Innate immune recognition of invasive bacteria accelerates atherosclerosis in apolipoprotein E-deficient mice. Circulation *109*, 2801-2806.

Green, P. H., and Glickman, R. M. (1981). Intestinal lipoprotein metabolism. J. Lipid Res *22*, 1153-1173.

Griffen, A. L., Becker, M. R., Lyons, S. R., Moeschberger, M. L., and Leys, E. J. (1998). Prevalence of Porphyromonas gingivalis and periodontal health status. J. Clin. Microbiol *36*, 3239-3242.

Guiney, D. G. (2005). The role of host cell death in Salmonella infections. Curr. Top. Microbiol. Immunol *289*, 131-150.

Hansson, G. K., Robertson, A. L., and Söderberg-Nauclér, C. (2006). Inflammation and atherosclerosis. Annu Rev Pathol *1*, 297-329.

Havel, R. J., Yamada, N., and Shames, D. M. (1987). Role of apolipoprotein E in lipoprotein metabolism. Am. Heart J *113*, 470-474.

Horai, R., Asano, M., Sudo, K., Kanuka, H., Suzuki, M., Nishihara, M., Takahashi, M., and Iwakura, Y. (1998). Production of mice deficient in genes for interleukin (IL)-1alpha, IL-1beta, IL-1alpha/beta, and IL-1 receptor antagonist shows that IL-1beta is crucial in turpentine-induced fever development and glucocorticoid secretion. J. Exp. Med *187*, 1463-1475.

Ishibashi, S., Herz, J., Maeda, N., Goldstein, J. L., and Brown, M. S. (1994). The two-receptor model of lipoprotein clearance: tests of the hypothesis in "knockout" mice lacking the low density lipoprotein receptor, apolipoprotein E, or both proteins. Proc. Natl. Acad. Sci. U.S.A *91*, 4431-4435.

Kanneganti, T. (2010). Role of NLRs in Innate Immunity and Disease. In (Banff, AB). Available at: http://www.stjude.org/stjude/v/index.jsp?vgnextoid=35880e03c7ec5110VgnVCM1000001e0215acRCRD&vgnextchannel=7cc71436e3218010VgnVCM1000000e2015acRCRD [Accessed June 25, 2010].

Kirii, H., Niwa, T., Yamada, Y., Wada, H., Saito, K., Iwakura, Y., Asano, M., Moriwaki, H., and Seishima, M. (2003). Lack of interleukin-1beta decreases the severity of atherosclerosis in ApoE-deficient mice. Arterioscler. Thromb. Vasc. Biol *23*, 656-660.

Kozarov, E. V., Dorn, B. R., Shelburne, C. E., Dunn, W. A., and Progulske-Fox, A. (2005). Human atherosclerotic plaque contains viable invasive Actinobacillus actinomycetemcomitans and Porphyromonas gingivalis. Arterioscler. Thromb. Vasc. Biol *25*, e17-18.

Kuramitsu, H. K., Chen, W., and Ikegami, A. (2005). Biofilm formation by the periodontopathic bacteria Treponema denticola and Porphyromonas gingivalis. J. Periodontol *76*, 2047-2051.

Lalla, E., Lamster, I. B., Hofmann, M. A., Bucciarelli, L., Jerud, A. P., Tucker, S., Lu, Y., Papapanou, P. N., and Schmidt, A. M. (2003). Oral infection with a periodontal pathogen accelerates early atherosclerosis in apolipoprotein E-null mice. Arterioscler. Thromb. Vasc. Biol *23*, 1405-1411.

Li, L., Messas, E., Batista, E. L., Levine, R. A., and Amar, S. (2002). Porphyromonas

gingivalis infection accelerates the progression of atherosclerosis in a heterozygous apolipoprotein E-deficient murine model. Circulation *105*, 861-867.

Lloyd-Jones, D., Adams, R. J., Brown, T. M., Carnethon, M., Dai, S., De Simone, G., Ferguson, T. B., Ford, E., Furie, K., Gillespie, C., et al. (2010). Heart disease and stroke statistics--2010 update: a report from the American Heart Association. Circulation *121*, e46-e215.

Martinon, F. (2007). Orchestration of pathogen recognition by inflammasome diversity: Variations on a common theme. Eur. J. Immunol *37*, 3003-3006.

Mattila, K. J., Pussinen, P. J., and Paju, S. (2005). Dental infections and cardiovascular diseases: a review. J. Periodontol *76*, 2085-2088.

Mayer-Barber, K. D., Barber, D. L., Shenderov, K., White, S. D., Wilson, M. S., Cheever, A., Kugler, D., Hieny, S., Caspar, P., Núñez, G., et al. (2010). Caspase-1 independent IL-1beta production is critical for host resistance to mycobacterium tuberculosis and does not require TLR signaling in vivo. J. Immunol *184*, 3326-3330.

Medzhitov, R., and Horng, T. (2009). Transcriptional control of the inflammatory response. Nat. Rev. Immunol *9*, 692-703.

National Institutes of Health (2010). Periodontal (Gum) Disease: Causes, Symptoms, and Treatments. Available at: http://www.nidcr.nih.gov/OralHealth/Topics/GumDiseases/PeriodontalGumDisease.htm [Accessed June 27, 2010].

Noach, L. A., Bosma, N. B., Jansen, J., Hoek, F. J., van Deventer, S. J., and Tytgat, G. N. (1994). Mucosal tumor necrosis factor-alpha, interleukin-1 beta, and interleukin-8 production in patients with Helicobacter pylori infection. Scand. J. Gastroenterol *29*, 425-429.

Paigen, B., Morrow, A., Holmes, P. A., Mitchell, D., and Williams, R. A. (1987). Quantitative assessment of atherosclerotic lesions in mice. Atherosclerosis *68*, 231-240.

Piedrahita, J. A., Zhang, S. H., Hagaman, J. R., Oliver, P. M., and Maeda, N. (1992). Generation of mice carrying a mutant apolipoprotein E gene inactivated by gene targeting in embryonic stem cells. Proc. Natl. Acad. Sci. U.S.A *89*, 4471-4475.

Plump, A. S., Smith, J. D., Hayek, T., Aalto-Setälä, K., Walsh, A., Verstuyft, J. G., Rubin, E. M., and Breslow, J. L. (1992). Severe hypercholesterolemia and atherosclerosis in apolipoprotein E-deficient mice created by homologous recombination in ES cells. Cell *71*, 343-353.

Portal-Celhay, C., and Perez-Perez, G. I. (2006). Immune responses to Helicobacter pylori colonization: mechanisms and clinical outcomes. Clin. Sci *110*, 305-314.

Priestle, J. P., Schär, H. P., and Grütter, M. G. (1989). Crystallographic refinement of interleukin 1 beta at 2.0 A resolution. Proc. Natl. Acad. Sci. U.S.A *86*, 9667-9671.

Qu, Y., Franchi, L., Nunez, G., and Dubyak, G. R. (2007). Nonclassical IL-1 beta secretion stimulated by P2X7 receptors is dependent on inflammasome activation and correlated with exosome release in murine macrophages. J. Immunol *179*, 1913-1925.

Rader, D. J., Alexander, E. T., Weibel, G. L., Billheimer, J., and Rothblat, G. H. (2009). The role of reverse cholesterol transport in animals and humans and relationship to atherosclerosis. J. Lipid Res *50 Suppl*, S189-194.

Rader, D. J., and Daugherty, A. (2008). Translating molecular discoveries into new therapies for atherosclerosis. Nature *451*, 904-913.

Reiss, A. B., and Glass, A. D. (2006). Atherosclerosis: immune and inflammatory aspects. J. Investig. Med *54*, 123-131.

Shaanan, B., Gronenborn, A., Cohen, G., Gilliland, G., Veerapandian, B., Davies, D., and Clore, G. (1992). Combining experimental information from crystal and solution studies: joint X-ray and NMR refinement. Science *257*, 961-964.

Stashenko, P., Gonçalves, R. B., Lipkin, B., Ficarelli, A., Sasaki, H., and Campos-Neto, A. (2007). Th1 immune response promotes severe bone resorption caused by Porphyromonas gingivalis. Am. J. Pathol *170*, 203-213.

Tabas, I. (2002). Cholesterol in health and disease. J. Clin. Invest. *110*, 583-590.

Takahashi, K., Takeya, M., and Sakashita, N. (2002). Multifunctional roles of macrophages in the development and progression of atherosclerosis in humans and experimental animals. Med Electron Microsc *35*, 179-203.

Tardif, F., Ross, G., and Rouabhia, M. (2004). Gingival and dermal fibroblasts produce interleukin-1 beta converting enzyme and interleukin-1 beta but not interleukin-18 even after stimulation with lipopolysaccharide. J. Cell. Physiol *198*, 125-132.

Vance, J. E., and Adeli, K. (2008). Assembly and secretion of triacylglycerol-rich lipoproteins. In Biochemistry of Lipds, Lipoproteins and Membranes (Elsevier), pp. 507-532.

Vigers, G. P., Anderson, L. J., Caffes, P., and Brandhuber, B. J. (1997). Crystal structure of the type-I interleukin-1 receptor complexed with interleukin-1beta. Nature *386*, 190-194.

Whitman, S. C. (2004). A practical approach to using mice in atherosclerosis research. Clin Biochem Rev *25*, 81-93.

Yamazaki, K., Honda, T., Domon, H., Okui, T., Kajita, K., Amanuma, R., Kudoh, C., Takashiba, S., Kokeguchi, S., Nishimura, F., et al. (2007). Relationship of periodontal infection to serum antibody levels to periodontopathic bacteria and inflammatory markers in periodontitis patients with coronary heart disease. Clin. Exp. Immunol *149*, 445-452.

Zhang, D., Lili Chen, Shenglai Li, Zhiyuan Gu, and Jie Yan (2008). Lipopolysaccharide (LPS) of Porphyromonas gingivalis induces IL-1β, TNF-α and IL-6 production by THP-1 cells in a way different from that of Escherichia coli LPS. Innate Immunity *14*, 99-107.

Zhou, Q., and Amar, S. (2007). Identification of signaling pathways in macrophage exposed to Porphyromonas gingivalis or to its purified cell wall components. J. Immunol *179*, 7777-7790.